

Biofuels

Implementation and Emissions Analysis

Daniel Wiznia

Garan Geist

Hiroataka Ellis

Advised by Professor Alessandro Gomez
Yale Department of Mechanical Engineering

New Haven, CT 06511

May 1, 2006

<u>IMPLEMENTATION AND EMISSIONS ANALYSIS OF BIOFUELS IN A COMBUSTION IGNITION LIGHT-DUTY VEHICLE</u>	3
1. INTRODUCTION	3
2. EXPERIMENTATION AND ANALYSIS	6
2.1 VEHICLE PREPARATION	6
2.2 PARTICULATE MATTER	8
2.2.1 Introduction to Particulate Matter Emissions	8
2.2.2 Experimental Apparatus for PM Measurement	8
2.2.3 Experimental Procedure for PM Measurement	11
2.2.4 Observations of PM	12
2.2.5 Discussion of PM Observations	14
2.2.6 Conclusion on Particulate Matter Emissions	16
2.3 CO AND NO _x	17
2.3.1 Introduction to CO and NO _x Emissions	17
2.3.2 Experimental Apparatus for Measuring CO and NO _x	17
2.3.3 Experimental Procedure for Measuring CO and NO _x Emissions	18
2.3.4 CO and NO _x Emissions Data	19
2.3.5 Observations on CO and NO _x Data	24
2.3.6 Analysis of CO and NO _x Trends	25
2.3.7 Conclusions on CO and NO _x Emissions	28
2.4 UNBURNED HYDROCARBONS	29
2.4.1 Introduction to HC emissions	29
2.4.2 Experimental Apparatus for Measuring HC Emissions	31
2.4.3 Experimental Procedure for Measuring HC Emissions	33
2.4.4 Observations of HC Emissions	36
2.4.5 Discussion of Observations for HC Emissions	41
2.4.6 Conclusions on HC Emissions	43
3. PROJECT CONCLUSIONS	44
ACKNOWLEDGEMENTS	44
APPENDIX A: RELEVANT INFORMATION FOR PM SECTION	45
APPENDIX B: RELATIVE INFORMATION FOR CO AND NO_x EMISSIONS	51
APPENDIX C: RELATIVE INFORMATION FOR HC EMISSIONS	52
APPENDIX D: ELECTROACOUSTICAL ESTIMATE FOR DAMPENING CHAMBER SIZE	57
APPENDIX E: IMAGES	59

IMPLEMENTATION AND EMISSIONS ANALYSIS OF BIOFUELS IN A COMBUSTION IGNITION LIGHT-DUTY VEHICLE

1. INTRODUCTION

Biofuels are a class of renewable fuels that derive from biomass – recently living organisms or their metabolic byproducts.¹ Our particular focus was on two varieties of biofuel: biodiesel and straight vegetable oil, both of which can be used to power a diesel engine with slight modification.

Biodiesel is a biofuel that has been refined to meet ASTM standards for diesel fuel. These standards state that biodiesel is a fuel composed of mono-alkyl esters of long chain fatty acids derived from vegetable oils or animal fats.² Biodiesel is typically produced by a reaction of a vegetable oil or animal fat with an alcohol such as methanol or ethanol in the presence of a catalyst to yield these esters and glycerin, which is then removed.³ Commercially available biodiesels are generally produced from soybean in the United States and rapeseed in Europe. Straight vegetable oil (SVO) is obtained by physically filtering used or unused vegetable oil. Though it can be easily obtained from restaurant waste, SVO requires more mechanical work to run properly in an engine.

Biodiesel has a higher cetane number than petroleum diesel, contains no aromatics, and contains 10% to 11% oxygen by weight. These characteristics of the fuel have been seen to reduce the emissions of carbon monoxide (CO), unburned hydrocarbons (HC), and particulate matter (PM) in the exhaust gas. However, studies have also shown that nitrous oxide (NO_x) emissions increase with the use of biodiesel.⁴ SVO has not been as extensively studied, so it has been included here in order to broaden the base of knowledge on another renewable energy source with potential to limit our dependence on fossil fuels.

The main difference between this study and most of those in the available literature is that actual on-road emissions were tested, whereas these previous studies used dynamometers to control engine loading. One interesting study that did test on-road emissions was conducted by the University of Denver. With a non-dispersive infrared component for CO, CO₂, and HC, together with a dispersive ultraviolet spectrometer for NO_x, the researchers were able to use their remote sensors to analyze the exhaust plumes of over 20,000 vehicles passing through a highway interchange over a three day period.⁵ While this study did not look at diesel fuel specifically, let alone biodiesel, it does show

¹ www.thefreedictionary.com/biofuel

² ASTM D 6751

³ National Biodiesel Board. “What is Biodiesel?”.
<http://www.biodiesel.org/resources/definitions/default.shtm>

⁴ Canakci, M. and J.H. Van Gerpen. “Comparison of Engine Performance and Emissions for Petroleum Diesel Fuel, Yellow Grease Biodiesel, and Soybean Oil Biodiesel.” 2003, American Society of Agricultural Engineers ISSN 0001-2351.

⁵ Pokharel, S., Bishop, G. and Stedman, D. “On-Road Remote Sensing of Automobile Emissions in the Denver Area: Year 3.” Coordinating Research Council. University of Denver. 2002.

that there is interest in learning about actual on-road emissions. Comparing our measured CO and NO_x emissions with the range of values found in the study, we can also see that our Suburban appears to be on the cleaner end of the spectrum (roughly 200 ppm NO_x on average for our truck vs. average values of 500 ppm in the study). Although this could be an effect of the terrain and loading conditions for their setup, it is at least good to see that our data values fall within the range of expected results.

While it is true that it is much simpler to create a repeatable experiment with the dynamometer, there exists the concern these results may not be truly representative of real driving conditions. By carefully constructing and refining the test procedures presented here, a comprehensive testing system that would not only be repeatable, but would allow the collection of accurate and meaningful results for biofuel emissions in our “moving lab” was developed.

The following tests focused on comparing emissions for four different fuels. First, the truck was run on regular petroleum diesel to obtain a baseline level for analysis. Two blends of biodiesel were then tested: B20 (a 20% biodiesel, 80% petroleum diesel mix) and B100 (100% biodiesel). A mixed blend allows biodiesel to be run safely at lower ambient temperatures, so a user will often run B20 in the winter, working their way up to B100 as the summer months come around. Mixing biodiesel with petroleum diesel is a relatively common practice for those in the biodiesel world, much as ethanol is beginning to be mixed in with gasoline at the pump for the everyday consumer. In fact, over 50 million miles of road testing has been done on B20 blends.⁶ It has been found from these tests that engine performance for biodiesel is very similar to that of petroleum diesels. Fuel economy, horsepower, and torque have not been shown to change by an amount greater than the variation found between different suppliers of petroleum diesel fuel, which can be up to 15%. The variations that have been noticed can be attributed to the slightly reduced energy content of biodiesel, which is on average 7-9% less than No. 2 diesel.⁷ Extensive analysis of stronger blends up to B100 has not yet been performed, but the results for B20 appear to carry over to these more concentrated blends. One concern on older vehicles is that the solvent nature of B100 will attack the fuel lines and seals, but this is not an issue for vehicles made after 1993, when new fuel line standards were instituted.⁸

Lastly, the vehicle was tested on straight vegetable oil, for which a special gas tank containing a heating element needed to be constructed. Because SVO is much more viscous than both the diesel fuel and biodiesel, it needs to be preheated to thin it out before entering the cylinder, which was accomplished by routing the engine coolant through the tank.

⁶ National Biodiesel Board Guidance: Nov. 30, 2005.

http://www.biodiesel.org/pdf_files/Biodiesel_Blends_Above%20_20_Final.pdf

⁷ Environmental Protection Agency. *A Comprehensive Analysis of Biodiesel Impacts on Exhaust Emissions*. US EPA Draft Technical Report 420-P-02-001; National Service Center for Environmental Publications: Cincinnati, OH, October 2002; <http://www.epa.gov/otaq/models/analysis/biodsl/p02001.pdf>.

⁸ National Biodiesel Board Guidance: Nov. 30, 2005.

http://www.biodiesel.org/pdf_files/Biodiesel_Blends_Above%20_20_Final.pdf

Additional concerns with biodiesel blends >20% include concerns over cold flow properties, materials compatibility, fuel stability, energy content, and engine oil dilution.

Test Property	No 2 diesel fuel ⁹	B100 used	Typical B100 (Soybean oil methyl Ester) ⁹	Typical SVO Soy Oil ¹⁰
Carbon (% mass)	86.66		77.00	
Hydrogen (% mass)	12.98		12.18	
Oxygen (% mass)	-		10.82	11.0
C/H Ratio	6.676		6.322	
Sulfur (% mass)	0.034	<.05	<0.005	0.01
Typical Formula	C _{14.01} H ₂₅		C _{18.74} H _{34.51}	
Average Molecular Weight	194.14		291.73 ^d	
Cetane Number (ASTM D613)	42.2	>47	50.4	38.1
Hydrocarbon Type, FIA (ASTM D1319)				
Saturates	56.6	-	-	
Olefins	1.6	-	-	
Aromatics	41.8	-	-	
Gross Heat of Combustion (Btu/lb)	19419		17183	
Net Heat of Combustion (Btu/lb)	18235		16072	40.81kJ/g
Specific Gravity	0.8559		0.8796	0.935
Kinematic Viscosity (@40°C, mm ² /s)	2.8911	4.201	4.5926	33.1
Total Glycerol (%)	-	.159	0.175	

Table 1 Fuel Composition

A few physical properties which are crucial for comparison between the fuels are cetane number and kinematic viscosity. These can be observed in Table 1. The cetane number of a fuel is an important characteristic that describes its ignition quality. For fuels with low cetane numbers and a long ignition delay, most of the fuel will be injected

⁹ Tat, M; Van Gerpen, J; Wang, P. "Fuel Property Effects on Injection Timing, Ignition Timing and Oxides of Nitrogen Emissions from Biodiesel-Fueled Engines". May 2006. Final Draft.

¹⁰ Demirbas, A. "Chemical and fuel properties of seventeen vegetable oils". *Energy Sources*, v 25, n 7. July, 2003. p 721-728

before ignition occurs, resulting in very rapid burning rates and correspondingly high rates of pressure increase and peak pressure. For a higher cetane fuel, ignition will occur before most of the fuel is injected. In this way, the heat release and pressure increase are controlled by the rate of injection and the fuel-air mixing, which results in smoother engine operation.¹¹ Biodiesel has longer chain alkanes and contains no aromatics compounds, both of which serve to increase the cetane number. However, there are disadvantageous physical properties of biodiesel. It has higher kinematic viscosity and surface tension, both of which influence atomization within the engine in a negative way.¹²

The chemical composition of SVO is somewhat tougher to determine. The oil that was used in the preliminary runs was waste fryer grease from the Yale dining halls. It was filtered and placed in settling tanks by David Johnson, a Research Support Specialist for the Chemistry department. This pulled out most of the food particulate matter from the oil, but the finished product was still quite raw in terms of refinement. Clearly, this fuel was much more irregular than the other fuels tested. However, due to an availability issue with the waste oil, pure soybean oil was acquired for the final test runs, purchased at a local supermarket. Chemically, these two fuels should be very similar, with the main difference being caused by any solid particles that may have passed through the filtering process of the waste oil.

Once the fuel choices for analysis had been made, the design process began on experimental systems for the determination of the amounts of major exhaust constituents produced by each fuel. The constituents that were chosen for study were particulate matter and soot, carbon monoxide, nitrous oxides, and unburned hydrocarbons. These choices were made because each of these compounds are currently regulated by law and are harmful to people and the environment.

2. EXPERIMENTATION AND ANALYSIS

2.1 Vehicle Preparation

In the spring of 2005, the Yale Engineering Design Team assembled a group of students who were interested in learning how to power automobiles with biofuels. The group prepared a biofuel project proposal with the support of Yale Engineering faculty, and the Mason Laboratory garage was provided as a storage space for the vehicle. This space proved to be invaluable because the research project's physical proximity to the faculty of engineering effectively reduced down-time spent in transportation to and from the vehicle. The space has also allowed for proper precautions to be implemented with regards to supervision. In its plan, the Yale Engineering Design Team satisfied all safety and insurance concerns held by the administration. The project was able to obtain over

¹¹ Heywood, John. *Internal Combustion Engine Fundamentals*. McGraw-Hill: New York, 1988.

¹² Lee, C.S; Park, S.W; Kwon, S.I. "An Experimental Study on the Atomization and Combustion Characteristics of Biodiesel-Blended Fuels". *Energy and Fuels*. American Chemical Society: 2005, 19, pp 2201-2208.

\$8000 of funding from the Yale Science Council, the Yale Faculty of Engineering, Biomedical Engineering, Mechanical Engineering, and Chemistry Departments. The suburban was purchased in the summer of 2005 and work began on the truck in the fall of 2005.

The 1991 suburban has an eight cylinder 6.5 liter diesel engine which has run for approximately 80K miles. In order to prepare for the test, two additional fuels tanks were added to the suburban. The first tank, the pre-heated straight vegetable oil tank, was fastened in the rear of the vehicle. To pre-heat the vegetable oil, hot coolant from the engine travels all the way back to the tank where it flows through a heat exchanger inside the fuel tank. The vegetable oil fuel line flows coaxially with the hot coolant, running countercurrent. In addition, the fuel passes through a heated filter before reaching the fuel pump. The second tank set-up that was installed allows for different biofuels to be selected for testing. With an under-hood toggle, switching between test fuels was relatively straightforward. Some of these modifications proved moderately challenging as installing new fuel lines incurred the risk of allowing larger air bubbles to form inside the fuel lines. As a result, fuel lines had to be filled with fuel by using a vacuum pump.

Many different problems were encountered during the installation and testing phases. These maintenance-related issues were frustrating because they caused setbacks in experimentation. During the fall of 2005 and spring of 2006, many hours were spent on the truck. The first road block occurred after the initial conversion, when a fuel line leaked a half gallon of diesel fuel onto the garage floor. This hazard, and the Safety Office's response, was a reminder to constantly monitor the truck and maintain safety procedures. Several other part failures developed over the course of the year. For example, the eight original fuel line return hoses began to fail after the conversion, creating numerous minor fuel leaks. Esters in the vegetable oil had destroyed the natural buna rubber hose. To correct the problem, the lines were replaced with a rubber synthetic.

One problem that has plagued the project has been fuel and coolant leaks. Because the vegetable oil is so corrosive, many of the original fittings would fail. In addition, because the conversion required many additional connections, there were more sites of possible failure. The group was required to replace many fittings that failed from exposure to biodiesel or poor connections. Because leaks continued to plague the project, close to half of the original modifications were overhauled with new hose or better fittings.

Because the vegetable oil runs coaxially through a coolant hose, special Swagelok fittings were required. The hoses heat up and cool down cyclically, so these fittings would begin to leak after a few uses and would require repairs. The truck also suffered a heater core leak. Because of time constraints, the heater core was not replaced, and instead was bypassed.

Because the vehicle did not come with a tachometer, a GTechPro Road Racer was installed. It provided the innovative reading of the car's engine speed through the cigarette lighter. The calibration of the tachometer function for this device was performed by visually matching engine speeds of the car with a variable frequency strobe light. Another capability of the Road Racer which turned out to be useful was its measurement of lateral and longitudinal acceleration. All data recorded by the Road Racer could store three hours of data that could be transferred to a computer for use in data analysis.

2.2 Particulate Matter

2.2.1 Introduction to Particulate Matter Emissions

Determining the level of particulate matter in the exhaust gas was both a difficult and interesting challenge. Particulate matter is an important property of exhaust gas to measure because soot has been implicated as a carcinogen. In addition, PM has been implicated as an initiator of asthma and respiratory illness. It is hypothesized that soot absorbs small molecules, which upon uptake by the body, releases these toxic substances into the bloodstream.¹³

When published, the Clean Air Act required lower emissions levels of PM. The EPA recommends that diesel vehicles older than 1990 emit exhaust lower than 55% opacity and vehicles 1991 and newer emit exhaust lower than 40%, with specific levels set by each state.¹⁴

Diesel PM is mainly carbon molecules which are a result of incomplete combustion of the fuel. At first small, the molecules gain in size as they collide to form larger masses. Particles of soot will grow as gaseous molecules incorporate into the particulate phase and when particles collide and form aggregates. The amount of PM is a good indicator of how efficient the fuels combusts.¹⁵

2.2.2 Experimental Apparatus for PM Measurement

An opacity meter was designed to measure the amount of particulates in the air. Opacity (N) is a light extinction measurement technique that quantifies the density of smoke exiting a vehicle, and an opacity rating will range between 0-100. $N = 100 * [1 - (I/I_0)]$ The darker the smoke, the more polluting the exhaust and the higher the opacity reading will be. Note that a Hartridge Smoke Meter Unit (HSU) is equivalent to percent opacity. Upon registering the Suburban, it was brought to a special diesel emissions center and received an opacity measurement of 19.6 when tested on a dynamometer, at normal road speeds for up to four minutes. In the state of Connecticut, the dynamometer runs a drive trace through higher (up to 40 mph) and lower speeds (idle) and the three highest opacity readings are recorded.¹⁶

The smoke meter was designed to adhere to the Society of Automotive Engineers J1667 recommended practice for smoke tests for heavy duty powered vehicles. The smoke meter was also designed to function during on-road tests. Before building the meter, an experimental setup was prepared in the laboratory. First, a red 680 nm laser was directed towards a photocell, which would create a small potential difference across the cell's leads. The voltage across the photocell was measured with a corded digital multimeter. In the lab, using a series of neutral density filters, varying intensities of light

¹³ EPA Cleaner Air Education Initiative. "Air Quality of Life". <http://www.aqol.org/brochure0404-AQOL.pdf>, 2003.

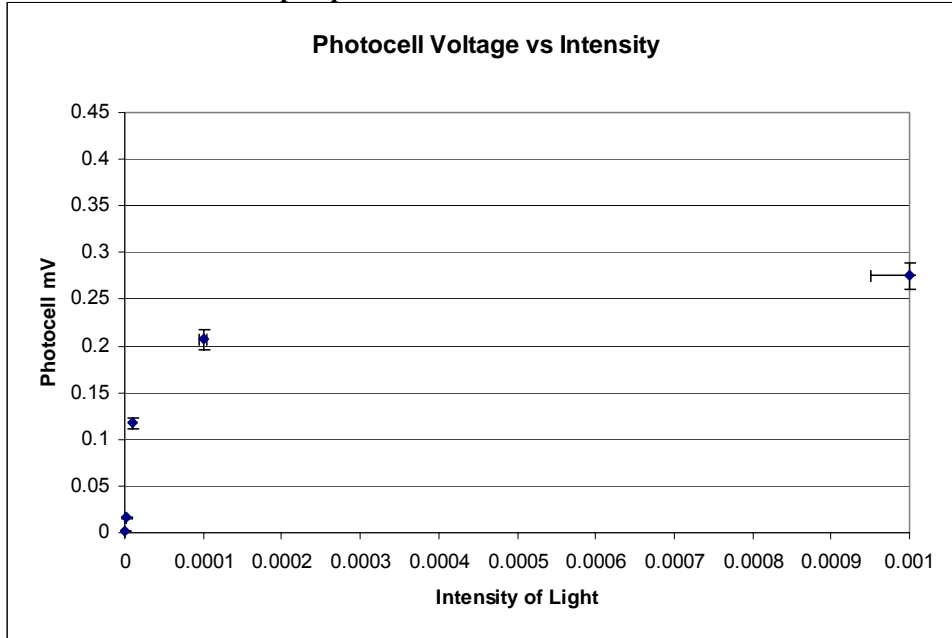
¹⁴ United States Environmental Protection Agency, National Vehicle and Fuel Emissions Laboratory. "Guidance to states on smoke opacity cutpoints". EPA420-F-99-024.

¹⁵ Heywood, J. *Internal Combustion Engine Fundamentals*.

¹⁶ Connecticut DMV, Diesel Emissions Testing Procedure.

were shined on the cell to calculate the cell's behavior. In the dark, the cell would output a potential difference of 0.000 mV while at high intensities, the cell would output approximately 0.400 mV. The relationship between light intensity and voltage turned out to be non-linear, but at very low light intensities, the photocell behaved linearly.

Figure 1: Non-linear relationship of photodiode



Because the laser was too bright, it was necessary to incorporate a system of neutral density filters into the design to lower the intensity of the laser beam. It was observed that ambient light in the room effected the voltage across the photocell. For example, a person walking by the meter displaced ambient light and the fluctuations could be observed in the output voltage. To reduce ambient effects, a red 680 nm filter was placed before the photocell. When the laser and photocell were taken to the garage bay to simulate the smoke meter, the sunlight saturated the photocell. Therefore, a permanent design had to enclose the meter from ambient light.

Because a 110V AC supply would not be available on the road, a battery powered voltmeter was used in place of the corded multimeter. In addition, a small pen laser was purchased to replace the large laser. Similar to pointers used during lectures, this laser could be operated using batteries. An assembly of 2 inch diameter black pipe was purchased to construct the assembly. Pipe was used because it ensured that the laser would be properly aligned with the sensor. A cross piece of pipe was used as a central hub. One female opening was attached to the tail pipe so that exhaust passed through the cross piece and exited through a 6-inch nipple. Two 4-inch nipples were attached perpendicular to the flow of exhaust. End caps were attached on both nipples to hold the photocell and the laser pointer. Both of these caps were machined so that the laser light would be focused directly onto the photocell.

Unfortunately, the system was initially plagued with problems. Neutral density filters had to be cut into fragments and stacked because the correct filters were not available. This stacking method produced reflections and increased background noise. In addition, the non-linearity of the photocell made readings difficult. Because the photocell only had a small linear range of 0.2V, the readings were terribly imprecise.

Several changes were made to the system to improve the faults. First, the photocell was replaced with a phototransistor. This allowed for a data acquisition device to log the data. In addition, the phototransistor had a linear range of over 2 volts, an order of magnitude larger than the photocell. Although the phototransistor required a power supply, the device was far more accurate and elegant. Data could be acquired at a very large frequency and recorded onto the computer.

In order to replace the crudely implemented neutral density filters, a high intensity bright LED was used. The LED was a great choice for several reasons. First, the brightness of the LED could be tuned to a value that complemented the phototransistor. This allowed for the filters to be removed. Second, the LED could be powered by the data acquisition card, and its behavior could be monitored with the computer. It took about a week to perfect the alignment and implement the new circuitry, but once built, the smoke meter worked very nicely and gave consistent readings. Both the LED and the phototransistor were connected to the A/D converter with BNC cables, and panes of microscope slides were used to protect the sensors from particulate matter. The panes of glass were glued in front of both the LED and the phototransistor so that the particulate matter would not settle on the surface of the sensors.

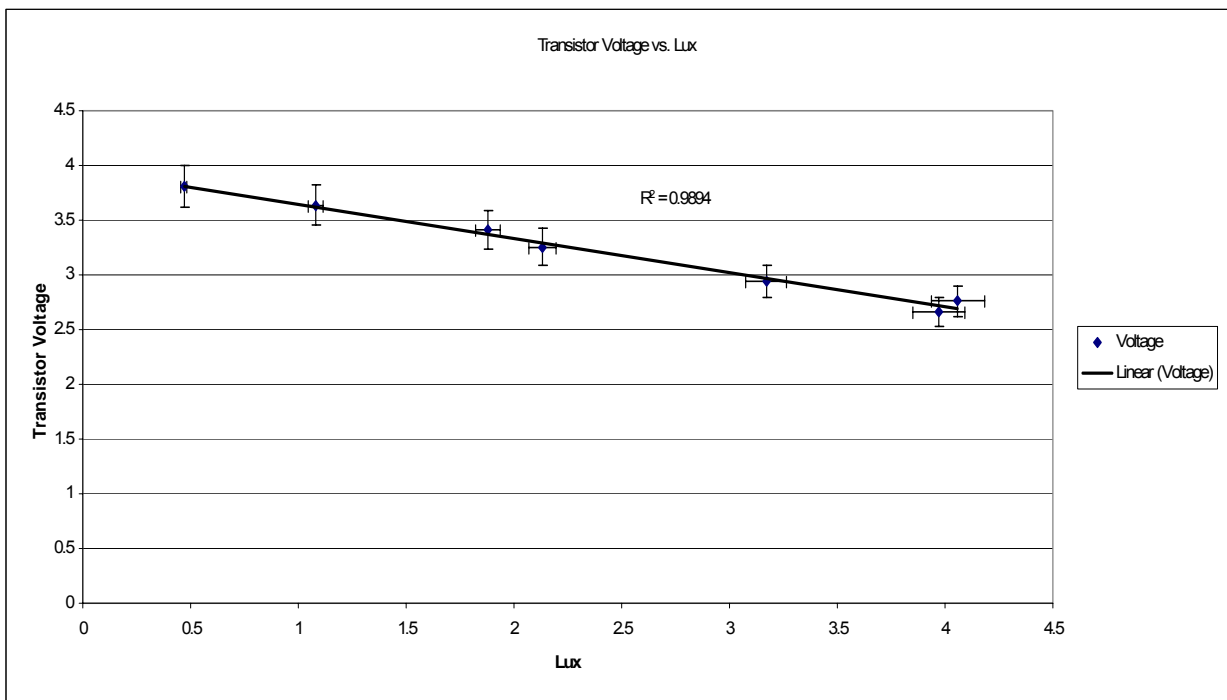


Figure 2: Linear relationship between LED and phototransistor

After testing the smoke meter, several new problems were introduced. First, when the smoke meter was used during road tests, particulate matter settled on the glass surfaces. In an attempt to reduce the accumulation of the soot, a series of baffles were placed within the nipples. Although the baffles greatly reduced the accumulation, a small film still formed. As an added benefit, the baffles prevented the nipples and the sensor packages from heating up from the exhaust. Next, a quarter-inch diameter copper pipe was inserted in the length of both nipples. The LED light was able to pass through the pipe. Again, although these pipes helped prevent soot from accumulating, there still was some soot accumulation on the glass over time. Unfortunately, it would be impossible to

use this system on the road because the soot did not accumulate in a linear fashion, but when the engine was placed under a load. Finally, air was blown from a compressor across the protective glass sheets. However, this was not a perfect solution; an air compressor and a battery pack had to be brought along for testing. Because the battery pack had a limited amount of power, the experiments can only be conducted for 15 minute sessions.

Finally, a flat black paint was applied to the surfaces of the pipes. This paint lowered background noise by reducing light from reflecting off of surfaces. In its final form, the opacity meter accurately collected data sets.

2.2.3 Experimental Procedure for PM Measurement

1. The computer and the Road Racer log data during the following tests. Hot start, two idle tests, Prospect, Edward, Canner, and two highway runs.
2. The truck is run for at least twenty minutes so that the engine reaches a steady running temperature.
3. The truck is turned off. Then, the truck is started.
4. The truck is run at idle for five minutes.
5. The truck is run taken up the Prospect street hill.
6. The truck is taken up the Edward street hill.
7. The truck is taken up the Canner street hill.
8. The truck is taken on I 91 for a five minute run.

[1] $T = I/I_0 = e^{-KL}$ **Equation 1**
 K = Light Extinction Coefficient
 L = Path Length (cm)

[2] **Opacity % = N = 100*(1-T)** **Equation 2**

Substitute [1] into [2]:
 [3] $N = 100*(1 - e^{-KL})$ **Equation 3**

Isolate K:
 [4] $K = [Ln(1-N/100)]/L$ **Equation 4**

if (T<553 Kelvin) Sp=86400 – constant for smoke density
 else if (T<623) Sp=348.13*T - 106117;
 else Sp=110769;

[5] **Soot Density (mg/m³) = (1E6*1000*K)/Sp** **Equation 5¹⁷**

[6] **Mass Fraction of Soot (mg/kg) =**
 $[(1E6*1000*K)/Sp]/[(101325*29/8314.34/T)]$ **Equation 6¹⁷**

¹⁷ DieselNet Technical Data Sheets. "Smoke Opacity Paper". www.dieselnet.com/calculator/smoke1/html

To be able to compare smoke opacity results from different vehicles, results have to be reported at the standard effective optical path length, 2 inches [51 mm]. The following equation is used to standardize results:¹⁸

$$[7] N_s = 100 * (1 - ((1 - (N_m / 100)) * (L_s / L_m))) \quad \text{Equation 7}$$

N_s = opacity, standard condition

N_m = measured value

L_s = standard optical path length

L_m = measured effective optical path length

The opacity meter was designed so the $L_s = L_m$, so equation [6] was not needed.

To be able to compare smoke opacity results from meters that have different light sources, smoke measurements were corrected with the following equation:¹⁹

$$[8] N_s = 100 * (1 - ((1 - (N_m / 100)) * (w_s / w_m))) \quad \text{Equation 8}$$

w_s = the wavelength of a standard green LED light source = 570 nm

w_m = the wavelength of a red LED light source = 660 nm

2.2.4 Observations of PM

Since a large amount of data was collected, only a summary is discussed below. Most satisfying are the data sets collected with the Road Racer and the opacity meter. The opacity meter collected data that is repeatable and substantial. Because the data sets for each test took a considerable amount of time to process, three tests were conducted for the diesel test to substantiate that the results are repeatable. In Figure 3, three diesel hot start tests can be observed. Although the tests appear to differ somewhat, each characteristic is within 1 or two percent from the average. For example, the hot start peaks are all within 2 opacity readings from the average (average = $29.28 \pm .54$, peaks = 30.85, 28.55, 28.45).

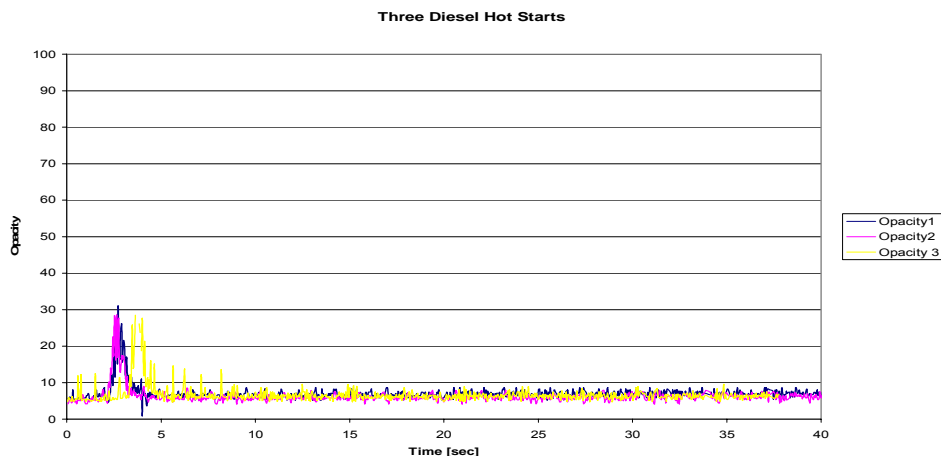


Figure 3: Demonstration of repeatability

¹⁸ Society of Automotive Engineers J1667 Recommended Practice Smoke Test Procedure

¹⁹ SAE J1667

Since the diesel tests continued to follow this pattern of repeatability, only two tests were conducted for each following fuels.

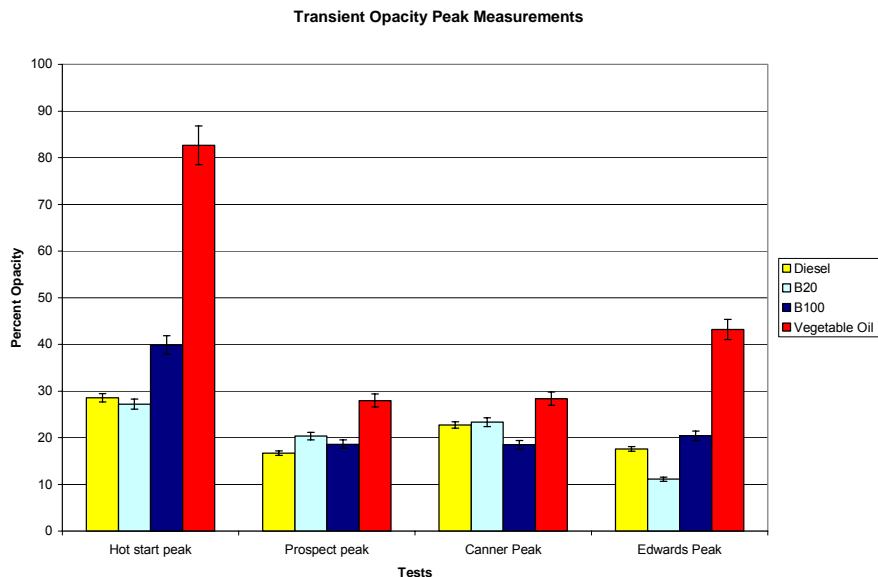


Figure 4: Transient observations There are two general tests, transient and steady state. First, the transient observations will be made. The largest opacity readings are consistently measured when the engine is accelerating (racing up a hill) or starting up. Within this subset of measurements, the highest opacity measurements are taken during the hot start test (82.67 ± 3.3 percent for vegetable oil and 27.16 ± 1.1 percent for B20). Consistently, straight vegetable oil has the highest opacity and diesel usually has the lowest. A general trend appears in which the fuel with the least amount of biofuel content (diesel) produces the least particulates during an acceleration of RPM. However, on both Canner and Edwards streets, the trend is not followed because B100 and B20 respectively break it.

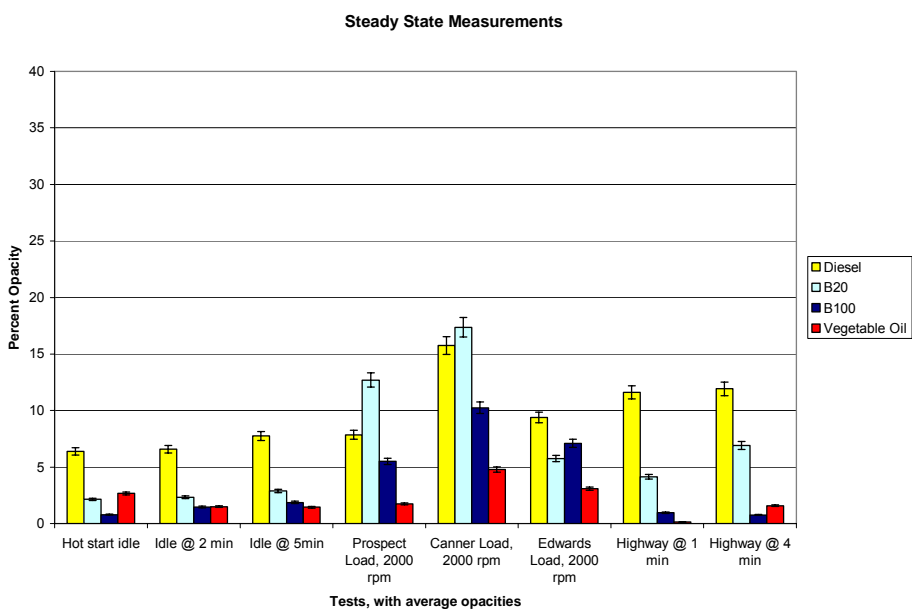


Figure 5

With the steady state data sets, it appears as though the opposite can be seen. Fuel which contains a higher percentage of biofuel (SVO) appears to emit less particulate matter. For example, the engine produced more particulate matter when it burned diesel than when it burned straight vegetable oil. In addition, more particulate matter is produced when the engine is under load than when it is in idle. For example, the engine produced more particulate matter when pulling the truck up Canner Street with steady rpms ($433 \pm 13 \text{ mg/m}^3$ with B20) than when in idle ($49.32 \pm 3 \text{ mg/m}^3$ with B20). The highway opacity readings are in between the opacity results for the idle tests and the hill tests. In summary, it appears as though fuels with more vegetable oil burn cleaner in the steady state but produce more soot in the transient state. However, it is important to note that some series of tests do not completely follow this trend.

2.2.5 Discussion of PM Observations

In many papers, it has been observed that fueling with bio based fuels reduces the PM emissions. Similarly, in our steady state tests, the biofuels produce fewer particulates, at times as much as 70 percent less between diesel and SVO. In addition, investigators have observed reductions in smoke density when using soy-derived biodiesel, sunflower-derived biodiesel and rapeseed-derived biodiesel.^{20, 21, 22} Since our vegetable oil is soybean oil, and our biodiesel blends are soy-derived, our data can be compared to these results.

There are several reasons why biofuels may burn cleaner than No. 2 Diesel. First of all, biodiesel and SVO contain 10-11 percent oxygen by weight.^{23,24} With petroleum diesel, most of the particulate matter forms because of incomplete combustion of fuel hydrocarbons.²⁵ However, with an oxygenated biofuel, it is thought that, during the combustion process, the presence of the oxygen in the fuel promotes more complete combustion. In each stage of the combustion process, oxidation can occur where carbon soot molecules or smaller carbon molecules are burned in the presence of oxygen to form CO and CO₂. According to Heywood, the yield of soot increases rapidly with increasing C/O ratio and is strongly enhanced by increasing pressure. Therefore, a lower C/O ratio should cause less particulates to form.²⁶ For instance, according to a study comparing shale oil to diesel fuel, shale oil produced a lower smoke opacity than diesel fuel. One factor suggested was that shale has a lower C/O ratio than diesel. The lower smoke

²⁰ Graboski, M. S. and McCormick, L. "Combustion of fat and vegetable oil derived fuels in diesel engines". *Prog. Energy Comb. Sci.*, 1998. vol. 24, pp. 125-164.

²¹ M. Ziejewski, K.R. Kaufman, A.W. Schwab and E.H. Pryde. "Diesel engine evaluation of a nonionic sunflower oil-aqueous ethanol microemulsion." *J. Amer. Oil Chemists Soc.* 61, 1984. pp. 1620-1626.

²² D.L. Reece and C.L. Peterson. "A report on the Idaho on-road vehicle test with RME and neat rapeseed oil as an alternative to diesel fuel". *ASAE Paper No. 93-5018*. ASAE, St Joseph, MI. 1993.

²³ Canakci, M. "Performance and emissions characteristics of biodiesel from soybean oil". Proceedings of the Institution of Mechanical Engineers. Part D, *Journal of Automobile Engineering* [0954-4070] yr:2005 vol:219 iss:7 pp:915 -922.

²⁴ Canakci, M; Van Gerpen, J. H. "Comparison of engine performance and emissions for petroleum diesel fuel, yellow grease biodiesel and soybean oil biodiesel". *Trans. ASAE*, 2003, 46(4), 937-944.

²⁵ Heywood

²⁶ Schumacher. "Heavy-duty engine exhaust emission tests using methyl ester soybean oil/diesel fuel blends". *Bioresource technology* [0960-8524] yr:1996 vol:57 iss:1 pg:31 -36.

opacity was attributed to more complete combustion of the fuel due to a higher content of oxygen in the shale oil composition.²⁷

Interestingly, one study suggests that there is a higher fraction of ultrafine particles and a lower fraction of fine particles in B20 when compared to diesel. This suggests that the lower opacity measurements for biofuels might be related to the particle size of the PM.²⁸

It is a bit more challenging to explain why higher particulates are seen in biofuels than in diesel during transient conditions. There are several hypotheses below that may help explain why.

First, biodiesel has a lower heating value when compared with diesel fuels (about 8-12% on average). In addition, vegetable oil has a heating content roughly 90% of No. 2 Diesel.²⁹ Therefore, all biofuels supply less energy per unit of mass when compared with diesel. When using a biofuel, it is necessary to inject more fuel into the cylinder to produce an equivalent amount of power. In itself, this might explain why more particulate matter is produced from biofuels. However, this theory does not fully explain the behavior, because the increase in particulate matter is only seen during a transient episode and not during steady state. From our observations, particulates are not higher with biofuels when the engine is under a high load at steady state. Interestingly, the biofuel's higher cetane number and oxygen content cause the fuels to ignite early. According to Heywood, early spark increases the amount of particulates because of incomplete combustion. Early injection or retarded injection timing also generally increases smoke (opacity versus injection timing forms a u-shape function, with a minimum at the optimized injection timing).

Another cause of the increase in particulates may be the difference in viscosities of the fuels. Biodiesel is a mixture of several fatty esters with each component contributing to the overall kinematic viscosity.³⁰ (see Table 1). Biodiesel's higher viscosity and specific gravity may affect the amount of fuel injected.³¹ Because biofuels are thicker, the injection pump may inject less fuel into the cylinder with each stroke. During a transient state, when the engine is accelerating, fuel that is less viscous may flow easier into the cylinder. While the injection system is designed to function with diesel's viscosity, it is not designed for the thicker biofuels.

Another possible cause of the increase in particulate matter in the transient state may be incomplete atomization, which leads to incomplete combustion. Particulate matter has been linked to incomplete combustion in the literature.³² Ideally, the fuel should be completely atomized to encourage efficient combustion. However, at low Reynolds numbers and high viscosities, the jet of fuel sprayed into the cylinder may not

27 G. Labeckas, S Slavinskas. *Energy Conversion and Management*. 46, 2005. pp. 139-150.

28 Turrio-Baldassarri. "Emission comparison of urban bus engine fueled with diesel oil and 'biodiesel' blend". *The Science of The Total Environment*. 2004. 327, issue 1. pp. 147 -162.

29 Agarwal. "Biodiesel development and characterization for use as a fuel in compression ignition engines." *Journal of Engineering for Gas Turbines and Power*, 2001. 123 issue 2. pp. 440 -447.

30 Knothe, G. "Kinematic viscosity of biodiesel fuel components and related compounds". *Fuel*, 2005. 84, issue 9. pp. 1059 -1065.

31 Canakci. "Performance and emissions characteristics of biodiesel from soybean oil"

32 Gomez. "Emission and performance characteristics of a 2 litre Toyota diesel van operating on esterified waste cooking oil and mineral diesel fuel". *Environmental Monitoring and Assessment*, 2000. 65, issue 1, pp. 13 -20.

atomize as well. According to past studies, biodiesel's higher viscosity and surface tension will affect spray pattern in the cylinder.³³ In addition, the viscosity of the fuel may affect the speed of the fuel being injected into the cylinder. Because of the higher viscosity of the bio-derived fuel, the jet may form large drops or drops with a wide range of sizes. The poor atomization affects the interaction of fuel and air in the chamber. For example, the particulate matter can be impacted by fuel-rich conditions that are a direct result of poor spray.³⁴ This may explain why particulate matter is increased in more viscous fuels.

2.2.6 Conclusion on Particulate Matter Emissions

Overall, it has been observed that biofuels produce less particulate matter than diesel when the engine is in a steady state. In fact, in the steady state, the amount of particulate matter appears to be reduced proportionally to the bio-derived fuel content. In contrast, it was observed that biofuels produce more particulate matter than diesel when the engine is in a transient state.

To confirm why these trends are observed it is necessary to conduct further experiments. First, the fuels could be pre-heated to different temperatures right before injection into the cylinders. This would allow the researcher to manipulate the viscosities and surface tensions of the fuels to determine which fuel properties are responsible for the soot. In addition, analysis of the quality of the atomization should be conducted to observe whether biofuels fail to atomize completely. It would have been very helpful for our experiments to have installed a fuel flow meter so that instantaneous measurements of the fuel flow could be observed. This would allow an investigator to see if increased fuel demand influences the soot. Finally, it would be interesting to be able to change the C/O ratio of the fuels to see if the oxygen content of the fuel truly influences the formation of particulate matter.

³³ Canakci. "Performance and emissions characteristics..."

³⁴ Lefebvre. "Atomization and Sprays". Routledge, Dec 1988. pp. 421.

2.3 CO and NO_x

2.3.1 Introduction to CO and NO_x Emissions

Measuring the carbon monoxide and nitrous oxide levels in the exhaust gas proved to be a challenging endeavor. These compounds are important to measure because of their high toxicity, and they can be detrimental to both people and the rest of our world. The main constituents of NO_x are NO and NO₂, which are linked to ground-level ozone formation, smog formation, and acid rain, and can even be deadly in high concentrations. At the levels that it is found in vehicle exhaust, NO_x is more likely to cause respiratory problems, such as asthma, coughing, or nausea.³⁵ CO is well-known to deprive the brain, heart, and other tissue of oxygen, which can lead to death.³⁶

2.3.2 Experimental Apparatus for Measuring CO and NO_x

With the assistance of David Johnson of the Chemistry department, a test meter capable of monitoring both CO and NO_x levels was procured. This Bacharach Portable Combustion Analyzer 65 utilizes a small pump to pull air from the exhaust stream into finely calibrated test cells, producing a digital readout of these exhaust constituents. However, before putting the Bacharach into practice, we first had to reconcile our use of the meter with its intended use.

The test meter is designed to operate on home and commercial furnaces. The probe is inserted into the ductwork, where a slow, steady stream of air passes across its tip.³⁷ Upon first receiving the meter, we tested it by sticking the probe tip right into the tailpipe of the vehicle. The meter could not handle these flow characteristics, and the CO and NO_x readings jumped around wildly, even at idle. Somehow, a means of dampening out the pulses in the exhaust, as well as slowing down the flow velocity to a value comparable to that of a furnace, had to be determined. Another challenge was designing a way to insert, operate, and remove the probe from inside the truck while on the road. All of these problems were solved with the design and construction of the dampening chamber.

Because the Suburban has a tailpipe on either side of the truck just behind the rear wheel, it was determined that the best place to attach some sort of buffering system would be on the back bumper. In this configuration, it could easily be attached to each tailpipe when need be, and would also allow access to the chamber through the rear window of the truck. Material selection was critical, because the chamber had to be designed not only to withstand the heat from the exhaust on the inside, but also to stand up against the elements and winds in excess of seventy miles per hour without springing a leak. It was also desirable to have a chamber that, while containing a large volume, would be very lightweight, for ease of installation and removal. After surveying the

³⁵ Fernando, S; Hall, C; Jha, S. "NO_x Reduction From Biodiesel Fuels". Department of Agricultural and Biological Engineering, Mississippi State University. *Energy & Fuels*, 2006. 20, pp. 376-382.

³⁶ Clean Air Council. "The Danger from Diesel". http://www.cleanair.org/Air/diesel_factsheet1_danger.pdf

³⁷ Bacharach Portable Combustion Analyzer. Instruction, Operation & Maintenance. 24-9219

available options, including pre-constructed steel tanks and large plastic coolers, it was determined that steel ductwork best fit the design criteria. Since it was designed for heating systems, temperature would not be an issue. It was also extremely lightweight, and a chamber could be designed to whatever size and shape necessary due to the interchangeability of straight segments, adaptors, tees, and reducers.

In order to size the chamber properly, an electroacoustical analysis was performed on the system. See Appendix D for this analysis.

Connecting the chamber to the tailpipes with flexible aluminum tubing helped to further dampen out exhaust pulses, as much of the unwanted energy went to vibrating the tubing. And because it was corrugated, flow resistance was further increased, helping to achieve the desired result. With a series of exhaust adaptors found at the local auto parts store and bolted onto the tailpipe itself, this 3” tubing was affixed to the exhaust pipe, and the dampening chamber was complete. Figure 5 below is an image of the actual



Figure 5: Dampening Chamber in Action

in all three planes, allowing for consistent probe placement in every test run. Another issue to be aware of was overloading of the test cells. Because an overload would render any collected data meaningless and potentially cause permanent damage to the probe, tests had to be limited to 5-10 minutes each, with time allowed for a purge cycle between subsequent runs.

apparatus. More images can be found in Appendix E at the end of the report.

Trial runs performed with the equipment produced encouraging results. The pulses were eliminated at the top of the chimney, and readings were stable during steady-state testing. However, we found it difficult to hold the probe in place in the stack, and it jostled around while on the road, affecting the results. For this reason, a bracket was created and attached to the stack. In combination with the Bacharach’s probe stop, this bracket effectively prevents probe movement

2.3.3 Experimental Procedure for Measuring CO and NO_x Emissions

In order to represent as broad a range of driving conditions as possible, three tests were planned. The first test monitored idle conditions. This test was chosen because much of a vehicle’s time is spent in idle and because it was the most easily repeatable test we could perform. An expressway test was also conducted, using the cruise control set at sixty miles per hour along a set course. The most intricate test performed was a city driving test. This test was run along a set course in downtown New Haven, incorporating a mix of stoplights, straight driving, and hills. By matching up the probe readings with the recorded RPM data from the GTech Road Racer, CO and NO_x emissions could be compared to loading conditions.

Procedure:

- 1) Turn on Bacharach, allow to warm up, begin running in ambient air. It is critical that warm-up period is performed with clean air (i.e. nowhere near running vehicle).
- 2) Ensure that truck is sufficiently warmed up and check exhaust tubing for any leaks.
- 3) Begin driving, insert probe through bracket and into chimney stack, tighten set screw. Allow probe to acclimate to exhaust stream for at least one minute or until steady.
- 4) Start recording on GTech and log first data point on Bacharach at same time. Take probe readings every 30 seconds at idle, every 20 seconds on highway, and every 15 seconds in the city.
- 5) After course has been completed, remove probe from stack and allow cells to purge for minimum of 5 minutes.
- 6) Perform next test. Change fuel and allow to cycle through lines if necessary.
- 7) Upload to computer and analyze data.

2.3.4 CO and NO_x Emissions Data

The first step in obtaining meaningful data for CO and NO_x emissions was to demonstrate the repeatability of the test results. Using the baseline petroleum diesel, each test was performed three times, on three different days with varying weather conditions. Figure 6 below shows the data for the idle test, which demonstrates acceptable repeatability within the range of the Bacharach meter (although error bars have been removed to avoid cluttering the data, all CO and NO_x readings with the meter are accurate to ± 10 ppm and ± 5 ppm respectively). Figures 7 and 8 plot the CO and NO_x readings for various highway runs, conducted on different stretches of road at a steady 60 mph. While the average values for each run match up, it was found that the repeatability greatly increased upon using the exact same route and cruise control settings for the highway test.

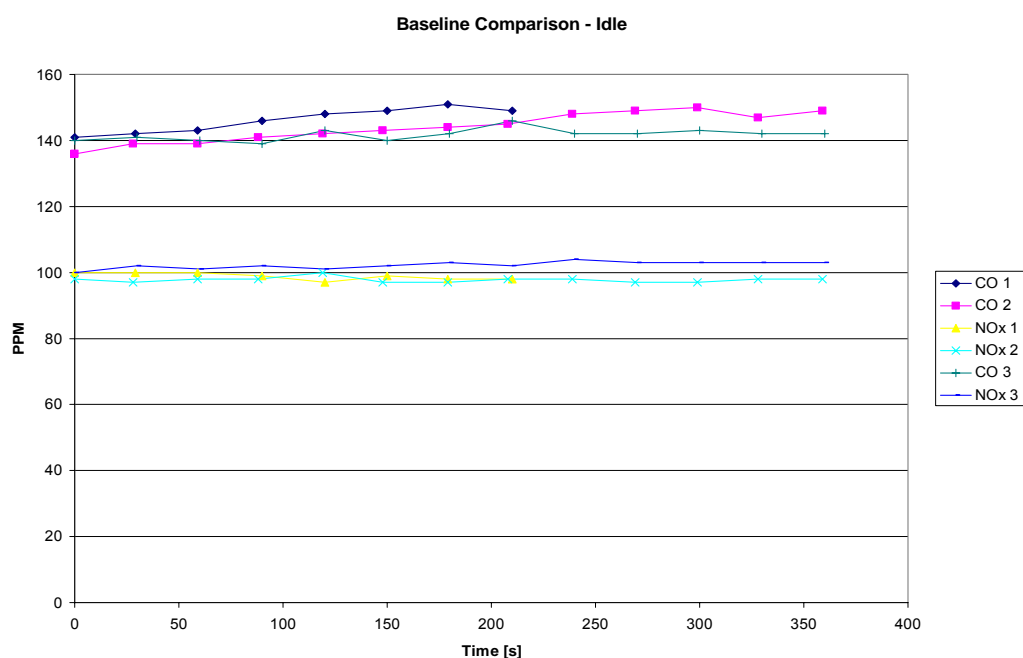


Figure 6

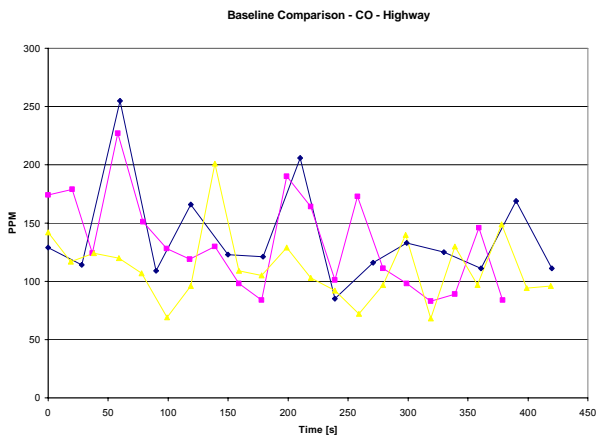


Figure 7

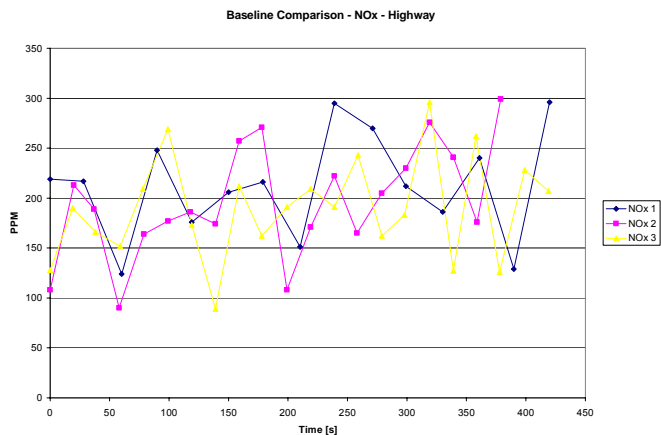


Figure 8

RPM and Longitudinal G's vs. Time - Highway Comparison

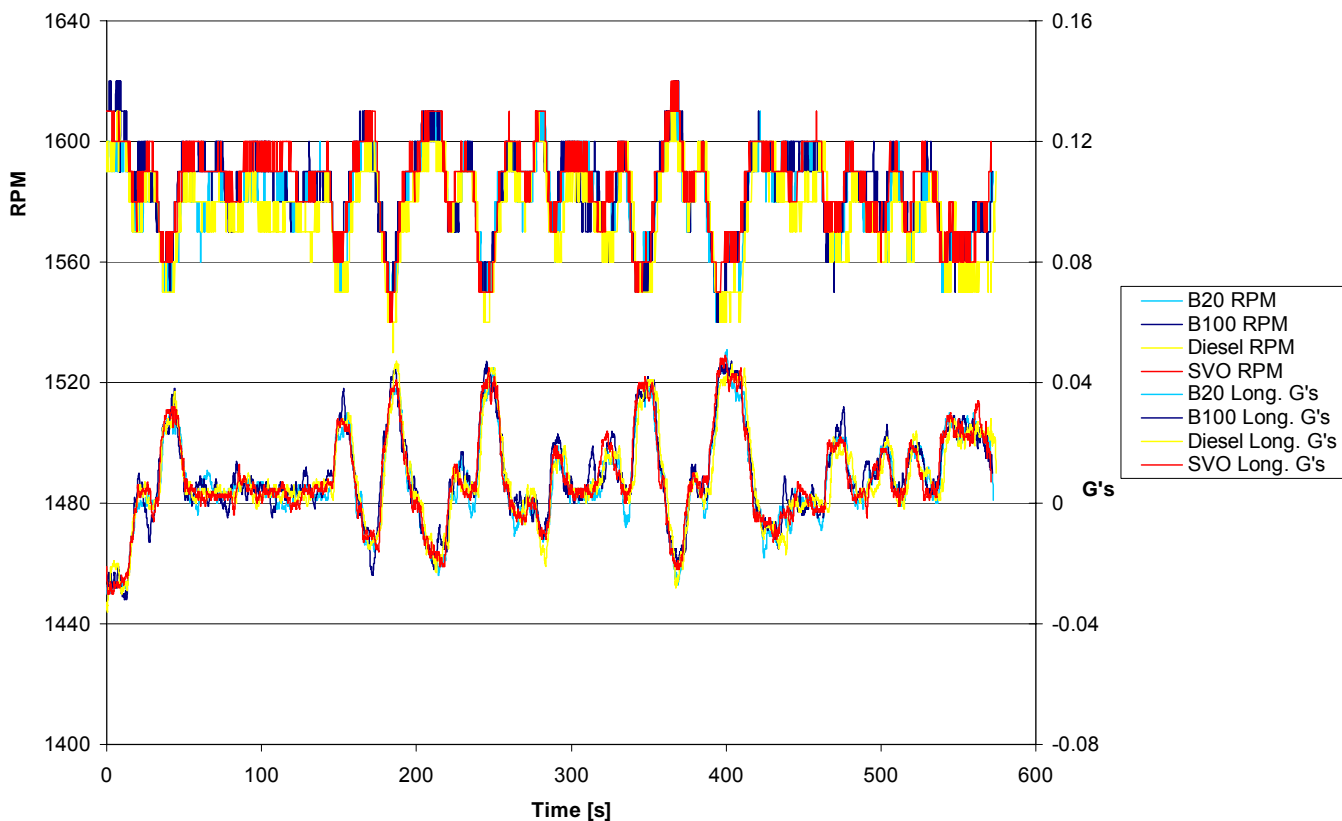


Figure 9

Figure 9 (above) shows the RPM data for these highway tests with the improved procedure. Clearly, the loading from trial to trial is quite consistent. Another helpful feature recorded by the GTech logger is the lateral and longitudinal g's. A positive value for the longitudinal g's means that the vehicle is slowing down, while a negative value implies acceleration. Using cruise control on the highway, this corresponds to traveling uphill and downhill, respectively. As shown by the overlay of the four runs plotted above, the timing of the test runs was extremely close. This guarantees that the corresponding probe measurements were taken at the same point along the road every time. Figures 10 and 11 below plot these CO and NO_x values for the highway runs.

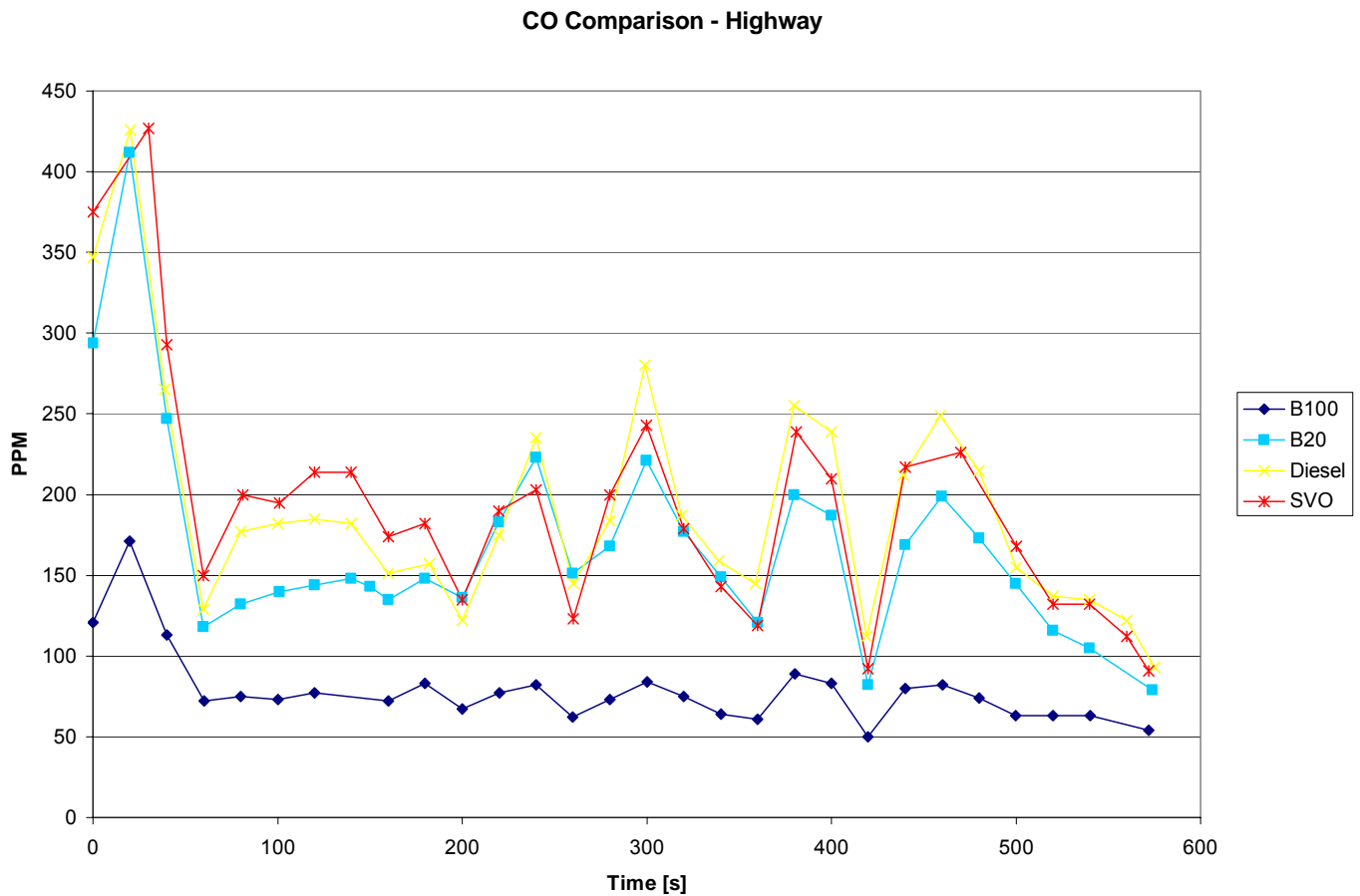


Figure 10

NOx Comparison - Highway

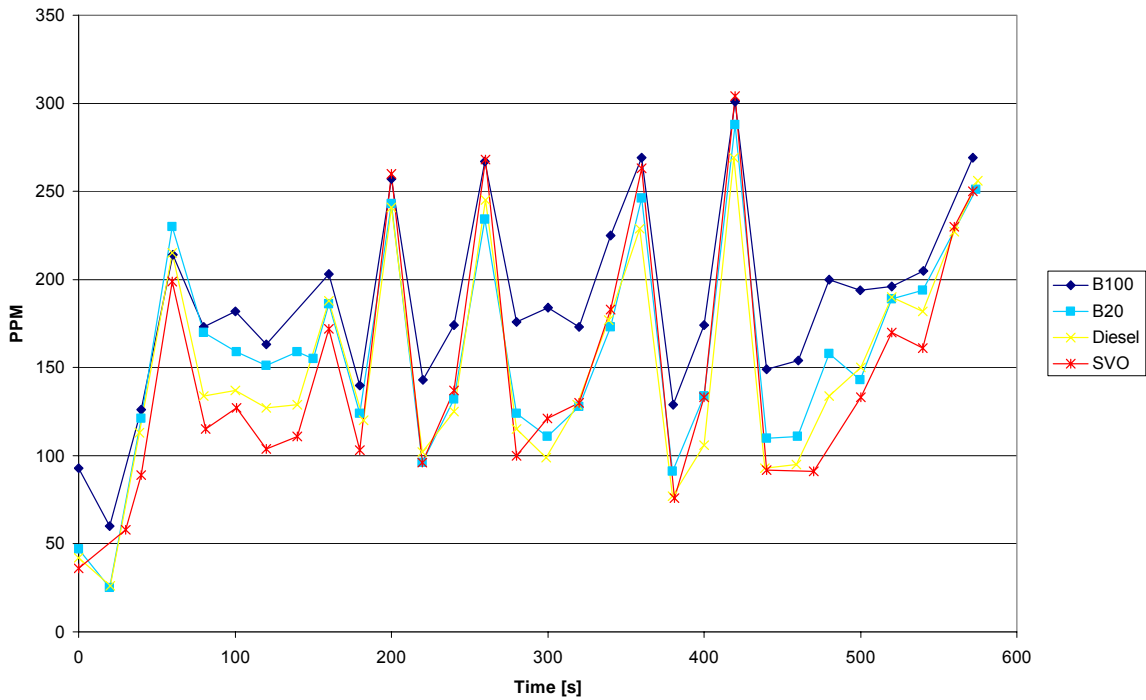


Figure 11

CO/NOx vs. Longitudinal G's - B100 - Highway

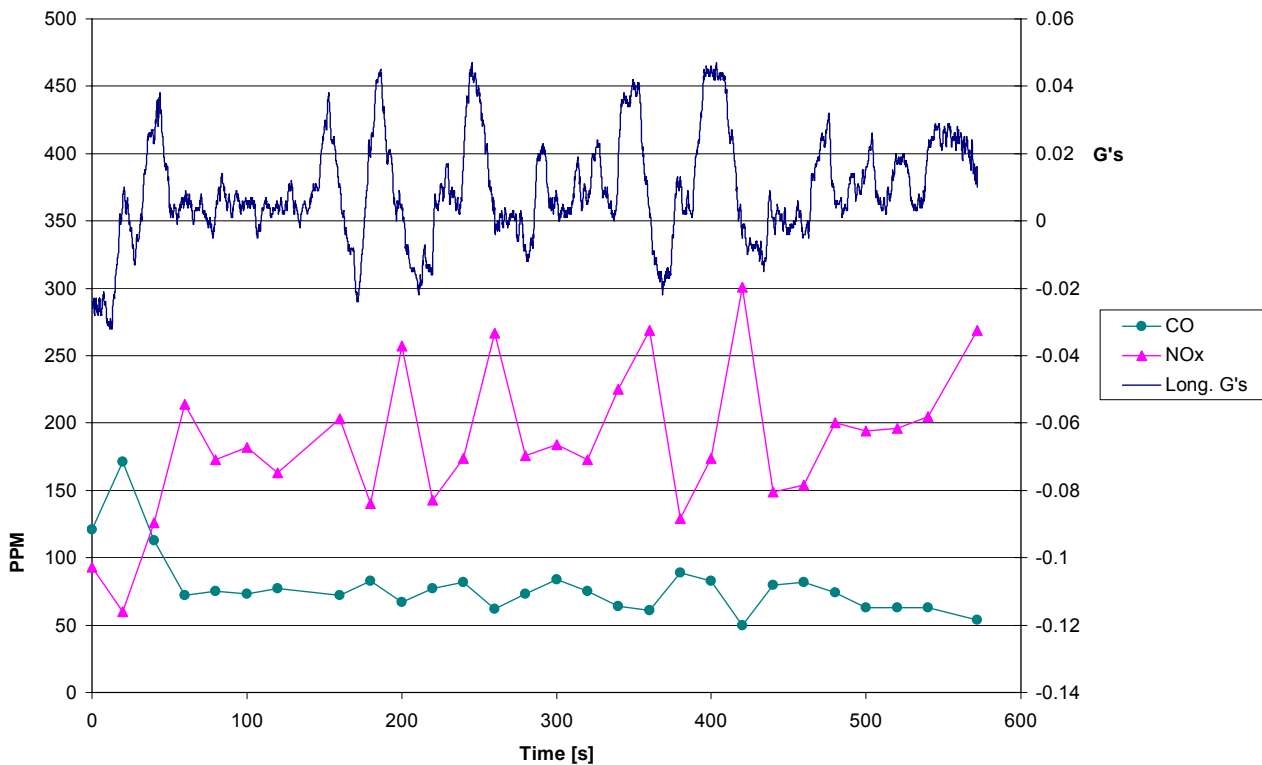


Figure 12

In Figure 12 (above), the longitudinal g's are plotted against the CO and NO_x emissions for the B100 sample. Reasons for the trend relating loading to the emission levels will be discussed in the analysis.

The results of the idle tests are reported below in Figures 13 and 14. These tests were conducted at an idle speed of 666 RPM, with the vehicle sufficiently warmed up and allowed to reach steady state.

Data for the city tests has not been presented in this report. The results from tests followed the general trends exhibited by the highway and idle tests, but were much messier due to the unpredictability of city driving. That being the case, including the plots here would only add unnecessary length while contributing nothing new to the scope of the project, and thus they have been omitted.

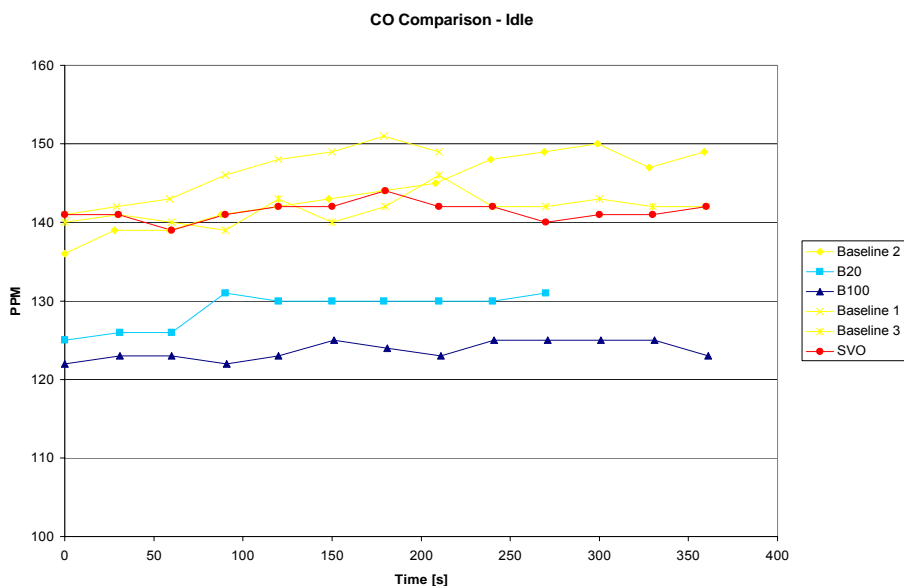


Figure 13

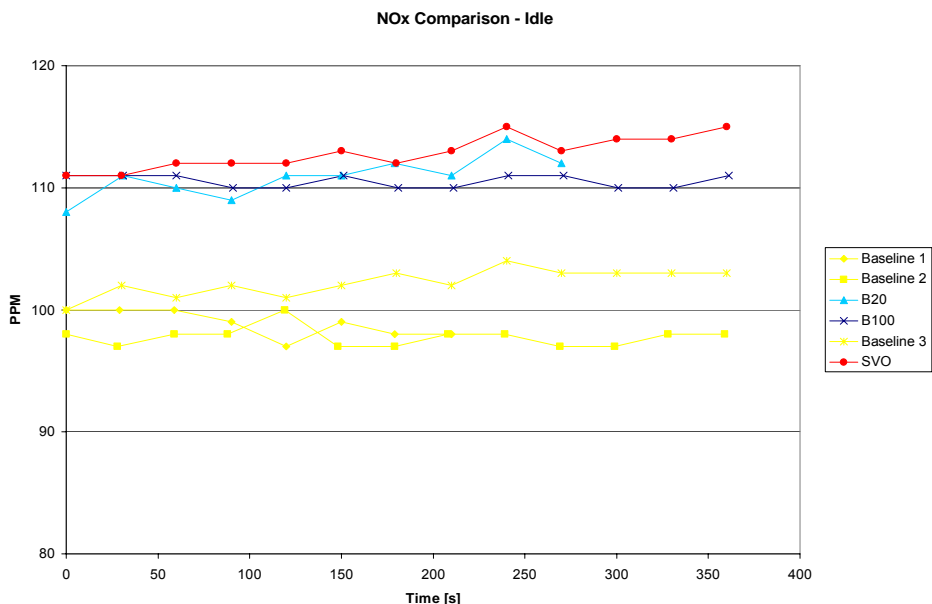


Figure 14

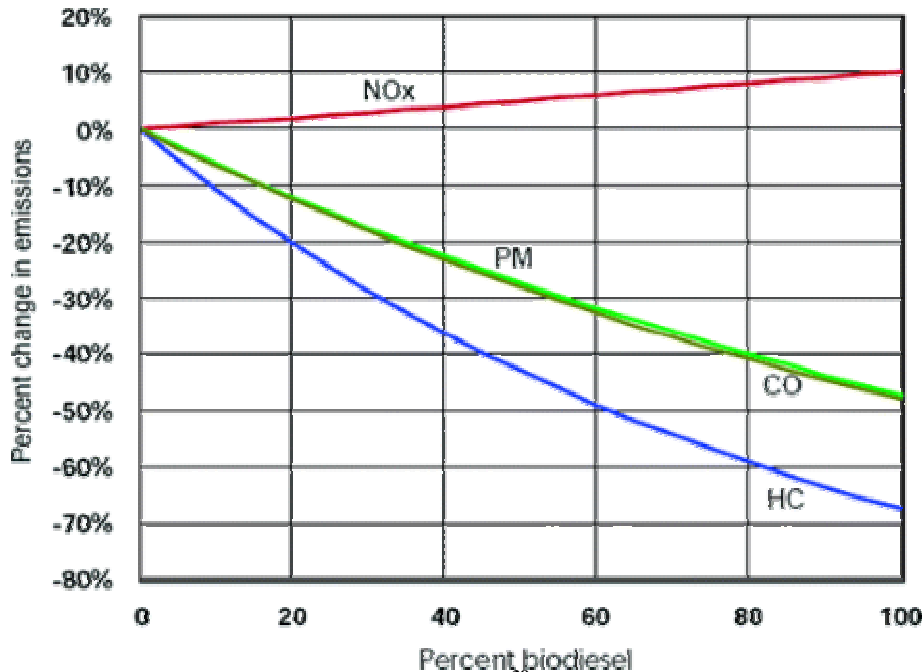


Figure 15³⁸

2.3.5 Observations on CO and NO_x Data

Figure 15 shows data from an EPA study on average emissions impact of biodiesel fuels for heavy-duty highway engines.³⁸ Important to note here is that, while biodiesel use reduces the levels of particulate matter, carbon monoxide, and unburned hydrocarbons in the exhaust, it has been found to increase emissions of nitrous oxides. These same trends have been exhibited in many other studies pertaining to biodiesel use in a range of different engines, fuel compositions, and operating conditions, with the exact value of the reduction or increase varying somewhat based on the specific experiment.

From a quick scan of the collected data, one can see that we too observed a reduction in CO emissions as well as an increase in NO_x with the use of biodiesel. At idle, we have found a significant reduction in CO (Figure 8) with the use of even just a 20% blend of biodiesel (roughly 10% reduction from an average value of 145 to 130 ppm). Although the reduction does not appear to have extrapolated linearly with the use of B100 fuel, we see that CO emissions do decrease further with pure biodiesel, to about 15%. As a tradeoff to the CO reduction at idle, we can also see the corresponding NO_x increase (Figure 9). For both B20 and B100 fuel, this increase was on the order of 10%. It is not clear why the increase in NO_x emissions for the B20 is as high as that for B100, but such small discrepancies have popped up in several places in this study, likely due to the limited number of trials run, as well as the many test factors beyond our control (weather, exact engine loading, etc). Although care was taken to limit testing variables as much as possible, the inherent difficulties of an on-road test procedure, in addition to the

³⁸ Environmental Protection Agency. *A Comprehensive Analysis of Biodiesel Impacts on Exhaust Emissions*. US EPA Draft Technical Report 420-P-02-001; National Service Center for Environmental Publications: Cincinnati, OH, October 2002; <http://www.epa.gov/otaq/models/analysis/biodsl/p02001.pdf>.

short amount of time available for the completion of the project, prevent us from going much further than a qualitative analysis of the data and the trends observed.

Several interesting things are going on in the highway tests. Looking at Figure 5, one can see a clear improvement in CO emissions after switching from petroleum diesel to B20 fuel. CO values peak at the same points along the road, but tend to be about 20% lower for the B20. The reduction seen with B100 fuel is even more drastic, so much so that the average CO value is less than half that of the baseline diesel (79 ppm compared to 192 ppm).

Figure 6 shows trends in the NO_x data matching that in the literature. With B100 use, the NO_x readings increase a significant amount, though not as much as the CO decreases. The emissions for B20, as one might expect, fall between those for petroleum diesel and B100, somewhat closer to the petrodiesel.

In Figure 12, one can see several trends that were not easily apparent in the other plots. As stated earlier, positive values for longitudinal g's represent uphill driving. Looking at the emissions for the B100 fuel, it is very clear that NO_x emissions are highest driving uphill, when the load on the engine is the greatest. There is also a noticeable offset of several seconds between the g-force peaks and the NO_x peaks, which can be explained by the time delay that exists for the exhaust traveling from the tailpipe up through the deadening chamber and out the chimney. Also evident on the plot is an inverse relationship between the NO_x and CO levels in the exhaust. A peak in the NO_x corresponds to a valley in the CO plot, and vice versa.

2.3.6 Analysis of CO and NO_x Trends

Now that the trends in the data have been pointed out, we seek to understand and explain the causes behind them. As mentioned earlier, Canakci and Van Gerpen state that the reductions in emissions are the result of biodiesel's higher cetane number, lack of aromatics, and 10-11% oxygen.³⁹ In a later study, Canakci reports that the different cetane number, heat of combustion, specific gravity, and kinematic viscosity of biodiesel influence the combustion and thus the engine performance, resulting in the NO_x increase⁴⁰, but this does not tell the whole story.

The CO, being the easiest to explain, is tackled here first. According to Heywood, in a fuel-rich spark-ignition engine, CO concentration will steadily increase. However, diesel engines always operate well on the lean side of stoichiometric, which means that CO emissions will be low, and regulations will easily be met.⁴¹ When one considers the chemistry of biodiesel, the CO emissions will be even lower. Because biodiesel is approximately 10% oxygen by weight, there will be extra oxygen to react with during the

³⁹ Canakci, M. and J.H. Van Gerpen. "Comparison of Engine Performance and Emissions for Petroleum Diesel Fuel, Yellow Grease Biodiesel, and Soybean Oil Biodiesel." 2003, American Society of Agricultural Engineers ISSN 0001-2351.

⁴⁰ Canakci, M; Erdil, A; Arcaklioglu, E. "Performance and Exhaust Emissions of a Biodiesel Engine". *Applied Energy*, Vol. 83. June, 2006.

⁴¹ Heywood, J. *Internal Combustion Engine Fundamentals*.

combustion process, allowing for more complete burning. In addition to reducing the amount of unburned hydrocarbons, this should reduce the emission of CO.⁴²

Furthermore, biodiesel has a lower carbon-to-hydrogen ratio than conventional petrodiesels. Lin and Lin found that biodiesel blends with the lowest carbon content formed the least CO, and all biodiesels emitted less CO than petroleum diesel.⁴³ This makes intuitive sense, because, with less carbon in the fuel, there is a better chance that each carbon atom will find two oxygen atoms to bind to.

The decrease in CO emissions that was noticed with an increase in loading can also be simply explained. When the load on the engine is higher, the gas inside the cylinder will naturally be at a higher temperature. This speeds up the conversion rate of CO to CO₂, completing the combustion process and lowering CO emissions.⁴³

The factors that go into NO_x formation are significantly more complex. First of all, NO_x can be split into three different forms, depending on how it is produced: thermal NO_x, prompt NO_x, and fuel NO_x.⁴⁴ Thermal NO_x is formed at high temperatures in the combustion chamber along the flame boundary, where oxygen combines with nitrogen from the air, following the extended Zeldovich mechanism.⁴⁵ The rate of this reaction is highly dependent on temperature, so that thermal NO_x production will speed up rapidly as the cylinder temperature increases.⁴⁴ This, then, explains why the NO_x values peaked sharply when the engine load increased on the highway test. Prompt NO_x forms as the result of hydrocarbon fragments reacting with nitrogen to form HCN, which then reacts with atmospheric nitrogen again to produce NO_x.⁴⁴ However, it has been found that prompt NO_x formation is only prevalent in rich combustion⁴⁶. Because diesels run lean, the prompt NO_x contribution will be small, and we can ignore it. The last kind of NO_x, fuel NO_x, forms when nitrogen in the fuel combines with excess oxygen during combustion. Because vegetable biodiesel contains no nitrogen, this component can also be disregarded.⁴⁴

Both Kanakci and Lin cite the oxygen content of the biodiesel as a reason why NO_x emissions increase.^{40, 43} They reason that because the fuel itself contains oxygen, there will be more oxygen available to react with the nitrogen in the air. However, Tat et al. state that the increase in NO_x is unexpected based on some of the biodiesel fuel properties, since a higher cetane number and lower energy content are usually associated with lower NO_x.⁴⁷ After combing through the literature, the NO_x increase appears to be a complex issue indeed, with several fuel properties combining with (and opposing) each other to obtain the final result.

⁴² Dorado, MP; Ballesteros, E; Arnal, JM; Gomez, J; Lopez, FJ. "Exhaust Emissions From a Diesel Engine Fueled With Transesterified Waste Olive Oil". *Fuel*, 2003; 82 pp. 1311-5.

⁴³ Lin, CY; Lin, HA. "Diesel Engine Performance and Emission Characteristics of Biodiesel Produced by the Peroxidation Process". *Fuel*, 2006; 85 pp. 298-305.

⁴⁴ Fernando, S; Hall, C; Jha, S. "NO_x Reduction From Biodiesel Fuels". Department of Agricultural and Biological Engineering, Mississippi State University. *Energy & Fuels*, 2006. 20, pp. 376-382.

⁴⁵ Bacharach, Inc. "Oxides of Nitrogen". 2005. <http://www.bacharach-training.com/combustionzone/nox1.htm>.

⁴⁶ National Energy Technology Laboratory. "Combustion NO_x Formation". Jan, 2005. www.netl.doe.gov/publications/proceedings/05/NOx_SO2/NOx%20Presentations/english_FosterWheeler_Zhi.pdf.

⁴⁷ Tat, M; Van Gerpen, J; Wang, P. "Fuel Property Effects on Injection Timing, Ignition Timing and Oxides of Nitrogen Emissions from Biodiesel-Fueled Engines". May, 2006. Final Draft.

Many studies of biodiesel combustion have found that the start of injection timing is advanced. This should result in a higher peak temperature inside the cylinder due to more premixed combustion, which will increase the rate of NO_x production. This will also result in a longer residence time, allowing NO_x production to continue for more time. In fact, this has been confirmed in a study by Szibist and Boehman, who found a linear trend between injection timing and NO_x emissions.⁴⁸ Of interest for the long-term viability of biodiesel use is a study that found NO_x emissions were actually less for biodiesel than for petroleum diesel when compared at the same injection and combustion timing.⁴⁹

Now that we know advanced injection timing is the likely cause of the NO_x increase, we seek to understand what is causing it. Fernando reports several factors that could all contribute to altering the timing. First, because the energy content of biodiesel is less than that of diesel, a greater volume of fuel must be injected to provide an equivalent torque, which will cause some injection pumps to advance their timing, following the engine's load-timing curve.⁴⁴ He also cites additional studies^{50, 51} which point out that biodiesel's higher speed of sound (allowing faster propagation of pressure waves) and greater bulk modulus (resulting in a more rapid pressure rise) may shift the injection timing settings from the optimized factory settings.

Tat et al. also report that the fuel's viscosity and density can have an effect on timing for fuel injection pumps with a hydraulically actuated timing mechanism. Attempting to isolate each potential factor, they concluded that the lower energy content, along with the higher bulk modulus, kinematic viscosity, and speed of sound all contributed to advancing the injection timing, while the higher density serves to retard the timing.⁴⁷ The overall effect is an advancement in the timing of 1-1.5°, depending on the specific fuel and pump used.

In addition to the injection timing, Tat et al. also looked at the ignition delay, and the cumulative effect these factors had on the combustion timing. Because biodiesel has a higher cetane number, it will have a shorter ignition delay, which advances the start of combustion even further (1.1° in the study). This results in a significantly longer residence time in the cylinder, causing higher NO_x emissions.⁴⁷ This result has also been corroborated by Szibist et al.⁵²

The straight vegetable oil is seen to produce slightly less NO_x than the baseline diesel while on the highway, but greater NO_x at idle. This is likely explained by the temperature inside the cylinder. Because SVO has a lower heat content than diesel, it will

⁴⁸ Szybist, J; Boehman, A. "Biodiesel Injection Timing Effects on NO_x Emissions". *Chem Phys Proc Combustion*, 2003. pp. 201-204.

⁴⁹ Monyem, A., Van Gerpen, J.H., and Canakci, M. 2001. "The Effect of Timing and Oxidation on Emissions". *Transactions of the ASAE*, Vol 44 (1), 2001. pp. 35-42.

⁵⁰ Tat, M; Van Gerpen, J. "The Kinematic Viscosity of Biodiesel and its Blends with Diesel Fuel". *Journal of American Oil Chem. Soc.*, 1999. 76, pp. 1511-1513.

⁵¹ Tat, M et al. "The Speed of Sound and Isentropic Bulk Modulus of Biodiesel at 21 °C from Atmospheric Pressure to 35 MPa". *Journal of American Oil Chem. Soc.*, 2000. 77, pp. 285-289.

⁵² Szybist, J; Boehman, A; Taylor, J; McCormick, R. "Evaluation of Formulation Strategies to Eliminate the Biodiesel NO_x Effect". *The Energy Inst, Penn State Univ. Fuel Processing Technology*, 2005. 86, pp. 1109-1126.

reach a lower peak combustion temperature.⁵³ Since the rate of NO_x formation is so dependent on temperature, this could lower NO_x emissions, even after factoring in the effects caused by any injection timing advancement. However, at idle speeds, peak temperatures will not be reached. At this state, the temperature inside the cylinder should be just as hot, and could actually be hotter for the SVO because it had to be preheated in order to lower the viscosity. This would explain the discrepancy, and in fact, the amount of preheating has been found to directly affect the NO_x emissions for waste frying oil.⁵³

CO emissions for SVO were found to be comparable to that of diesel at both idle and highway loading. Although one might expect the CO emissions to be lower due to the presence of oxygen in the fuel, as is the case with biodiesel, the extremely high viscosity of the vegetable oil will be working counter to this trend. Atomization and spray characteristics will be poor, which can create locally rich air-fuel mixtures. This in turn will increase the CO formation.⁵³ It appears that, for our particular set-up, these effects have roughly cancelled each other out.

2.3.7 Conclusions on CO and NO_x Emissions

The high level of NO_x emissions is the major obstacle standing in the way of broad support for biodiesel, and much research has been devoted to its reduction, particularly in light of stringent exhaust emission regulations being imposed on diesel engines over the next few years. One popular method of reducing NO_x emissions is exhaust gas recirculation (EGR).⁵⁴ EGR reduces engine temperature by pumping a portion (10-25%) of exhaust gas back into the intake. Because the exhaust gas is nearly inert, it will not react in the combustion chamber and acts only as a heat sink.⁵⁵ A small power loss is associated with EGR systems, but NO_x emissions are decreased by up to 80%.⁴⁴

Another option to reduce NO_x emissions is to install a catalytic converter. However, they work best at the stoichiometric ratio, so it will not be as effective on a diesel engine. They are also expensive and work better at high temperatures, while diesel exhaust is generally lower than gasoline exhaust.⁴⁴ Selective noncatalytic reduction, diesel oxidation catalysts, water-fuel emulsions, and NO_x and particulate traps have also been used to reduce NO_x emissions on biodiesel engines.^{44, 54}

All of these methods, however, are only solving the problem of biodiesel NO_x emissions indirectly, by removing the NO_x after it is created. It is our recommendation that future effort be directed at the major cause of the higher NO_x levels: the injection timing advancement. As mentioned earlier⁴⁹, returning the injection timing to its optimized setting will result in decreased NO_x emissions for biodiesel when compared to petrodiesel. Thus, in order for biodiesel to become a more viable alternative fuel in the

⁵³ Pugazhivadivu, M; Jeyachandran, K. "Investigations on the Performance and Exhaust Emissions of a Diesel Engine Using Preheated Waste Frying Oil as Fuel." Dept. of Mech. Eng, Pondicherry Engineering Collge. *Renewable Energy*, 2005. 30, pp. 2189-2202.

⁵⁴ Knothe, G; Sharp, A; Ryan, T. "Exhaust Emissions of Biodiesel, Petrodiesel, Neat Methyl Esters, and Alkanes in a New Technology Engine". National Center for Agricultural Utilization Research, USDA. Engine and Vehicle Research Division, Southwest Research Institute. *Energy & Fuels*, 2006. 20, 403-408.

⁵⁵ Chevron. "Emission Reduction Technologies". 1998.
http://www.chevron.com/prodserv/fuels/bulletin/diesel/L2_6_9_rf.htm

future, engine companies must plan for its use and design their injection systems accordingly. If the engine can be programmed to recognize and optimize for its use, there will be no downside to using a domestic, renewable, and cleaner-burning fuel such as biodiesel.

2.4 Unburned Hydrocarbons

2.4.1 Introduction to HC emissions

Another regulated emission from automobiles is hydrocarbons. Several previous studies have reported their observations of the total hydrocarbon emissions of various types of engines running on biofuels. Naturally, their results for these fuels are compared with that of conventional petroleum diesel fuel for the purpose of evaluating their value as an alternative fuel. There is an overall trend that can be studied with the use of biodiesel and biodiesel blends – engines running on this refined biofuel generally decreases total hydrocarbon emission compared to petrodiesel.^{56, 57, 58} For engines fueled with waste vegetable oils (before transesterification) and its blends, previously reported emissions results are mixed. Some claim decreased pollutant emissions while others claim increases.⁵⁹ Waste vegetable oil composition varies from batch to batch; this is visible from the varying colors that can be seen in the waste oil used in Yale biofuel applications.

Less frequently, one comes across a study of individual species of hydrocarbons in automobile emissions. The hydrocarbon family of chemical species includes various compounds, some of which are toxic. The known toxins of interest as suggested by the EPA's report on biodiesel exhaust emissions are known as mobile source air toxics (MSATs). These are suspected to cause cancer, and can have other harmful consequences as well. Table 2 displays a list of toxic compounds introduced in the EPA report.⁶⁰

⁵⁶ L. G. Schumacher, "Heavy-duty engine exhaust emission tests...".

⁵⁷ A. Tzolakis, A. Megaritis. "Exhaust gas assisted reforming of rapeseed methyl ester for reduced exhaust emissions of CI engines". Elsevier: Birmingham. *Biomass and Bioenergy*, 2004. Vol. 27, pp 493-505.

⁵⁸ Canakci, "Performance and emissions characteristics of biodiesel from soybean oil".

⁵⁹ M. Canakci et al. "Comparison of Engine Performance and emissions ..."

⁶⁰ EPA. "A Comprehensive Analysis of Biodiesel ...".

Table 2 List of MSATs

Acetaldehyde Acrolein Arsenic Compounds ¹ Benzene 1,3-Butadiene Chromium Compounds ¹ Diesel Particulate Matter + Diesel Exhaust Organic Gases (DPM + DEOG) Dioxin/Furans ² Ethylbenzene Formaldehyde	n-Hexane Lead Compounds ¹ Manganese Compounds ¹ Mercury Compounds ¹ MTBE Naphthalene Nickel Compounds ¹ POM ³ Styrene Toluene Xylene
<p>¹ Although the different metal compounds generally differ in their toxicity, the onroad mobile source inventory contains emissions estimates for total metal compounds (i.e., the sum of all forms).</p> <p>² This entry refers to two large groups of chlorinated compounds. In assessing their cancer risks, their quantitative potencies are usually derived from that of the most toxic, 2,3,7,8-tetrachlorodibenzodioxin.</p>	<p>³ Polycyclic Organic Matter includes organic compounds with more than one benzene ring, and which have a boiling point greater than or equal to 100 degrees centigrade. A group of seven polynuclear aromatic hydrocarbons, which have been identified by EPA as probable human carcinogens, (benz(a)anthracene, benzo(b)fluoranthene, benzo(k)fluoranthene, benzo(a)pyrene, chrysene, 7,12-dimethylbenz(a)anthracene, and indeno(1,2,3-cd)pyrene) are used here as surrogates for the larger group of POM compounds.</p>

From this list, the EPA studied eleven known emissions of biodiesel exhaust and correlated the emission of these compounds to total hydrocarbon emission measurements as well as to the percentage of biodiesel by volume in standard diesel. The EPA suggests that higher biodiesel content of fuel resulted in lower hydrocarbon and MSATs emissions. Though the actual correlation of MSATs emissions to total hydrocarbon emissions has yet to be thoroughly investigated, it seems that decreased overall HC emissions from automobiles goes hand-in-hand with decreased toxicity due to MSAT hydrocarbons.⁶¹ This government report confirms the validity of studying total hydrocarbon emissions in the observation of the hydrocarbon toxicity of automobile exhaust.

Hydrocarbons are also a contributing factor in the creation of smog and ozone.⁶² Hydrocarbon emission, also called volatile organic compound (VOC) in atmospheric chemistry, is the main ingredient to the creation of photochemical smog. The oxidation reaction of the VOCs leads to the creation of ozone and aldehydes. Aldehydes are among the MSATs discussed previously. The product ozone is also toxic. Ozone has poor solubility properties which, when taken into the lungs, can cause inflammation due to oxidization of lung tissue. The consequences of local ozone formation also include detrimental effects on crop yields and the faster wearing of tires. When hydrocarbons are combined with NO_x emissions, more volatile reactions resulting in ozone formation are possible.⁶³ NO_x emissions, described in the previous section, are an important emission of automobile exhaust. The reduction of hydrocarbons effectively means a reduction of many harmful consequences of hydrocarbon release into the environment.

⁶¹ “EPA, “A Comprehensive Analysis of Biodiesel ...”.

⁶² “Biodiesel Emissions,” National Biodiesel Board, http://www.biodiesel.org/pdf_files/fuelfactsheets/emissions.pdf

⁶³ Schade, G. “Photochemical Air Pollution I.” Lectures for Advanced Atmospheric Chemistry, March 28th, 2006.

2.4.2 Experimental Apparatus for Measuring HC Emissions

In order to measure hydrocarbon emissions from the Yale biofuel vehicle running various fuels, a flame ionization detector (FID) was used. There were two main driving factors in the initial choice of the use of a FID. The first was financial – this study was limited by a small budget which, given the comparably exorbitant prices of gas analysis and sampling equipment, prevented the purchase of new gas analyzers. The other reason was availability. The Horiba FIA-220 FID analyzer was sitting in storage at the Yale Engineering Center for Combustion Studies and was an easy acquisition for use with this project.

Flame ionization utilizes a hydrogen flame to convert the carbon content of a sample gas into a voltage reading. When a gas with organic content is added to flame fuel, H_3O^+ is formed by proton abstraction from CHO^+ . Space charge theory is then used to explain the relation between the current extracted from the flame and its related voltage.⁶⁴ The flame ionization detector is a popular analyzer for examining organic content in gases due to its linear output and ease of use.⁶⁵

Its popularity is unchallenged in the area of automotive exhaust analysis. The flame ionization detection process for automobile exhaust gases is expressed in terms of an equivalent concentration of propane. Output is in terms of parts per million carbon equivalent. Since all other hydrocarbons will not have quite the same response per unit carbon, the FID adjusts for these with relative correction values. In the end, though, its output is not an exact reading of the hydrocarbon content of gases but is an approximation.⁶⁶ To demonstrate its effectiveness in this approximation, Schofield analyzed two sample exhaust gases. His FID mass readings and their closeness to the actual mass of the hydrocarbons calculated from the chemical composition of the gas “illustrate how remarkably well suited the FID is for realistically integrating the concentration and mass of the complex hydrocarbon mixture emitted from internal combustion engines.”⁶⁷

There are two main types of flame ionization detectors – heated and unheated. The Horiba FIA-220 analyzer is an unheated flame ionization detector. There are disadvantages to using an unheated FID over a heated analyzer. The primary problem is that because it operates at ambient temperature, there is an issue of water condensation. Water, as a primary product of combustion, is abundant in automobile exhaust gas. According to Doug Miller, technical support at Horiba USA, the problem with water existing in the gas sample is two-fold. First, water condensation, which will occur due to the ambient temperature of the analyzer, will cause flow problems. Second, the water solubility of some of the heavier hydrocarbons will result in a lower than expected reading of hydrocarbon concentration. Schofield’s study (cited above) compares the performance of heated and unheated FIDs in analyzing automobile exhaust and comes to

⁶⁴ H. C. Bolton, Janine Grant, I.G. McWilliam; A.J.C. Nicholson, D.L. Swingler. “Ionization in Flames II”. Proceedings of the Royal Society of London. Series A, *Mathematical and Physical Sciences*, JSTOR: 1978. Vol. 360, No. 1701.

⁶⁵ “Flame Ionization” <http://www.instrumentalchemistry.com/gasphase/pages/fid.htm>.

⁶⁶ Schofield, K, “Problems with Flame Ionization Detectors in Automotive Exhaust Hydrocarbon Measurements,” *Environmental Science and Technology*, 1974, Vol. 8, No. 9.

⁶⁷ Schofield, “Problems with Flame Ionization Detectors...”

a similar conclusion. He observes that the difference between the heated and unheated FID is more pronounced when the exhaust contains more toluene, a heavier hydrocarbon. Schofield raises the possibility that the differences in the FID outputs in his study may not have come from reduced absorption and condensation of heavier hydrocarbons with higher boiling points but may be a result of different relative molar sensitivities to the hydrocarbon species.⁶⁸ The conclusion drawn from this information is that, although the FIA-220 is not a heated FID, its use should not be ruled out for this study.

Since the analyzer itself cannot counteract the water in the exhaust, the sampling system had to account for this problem. Other factors which affected the sampling system design were the fact that all emissions testing was performed in on-road situations (as opposed to stationary dynamometer testing) and that the FID setup is not portable. In order to address the water in the sample line, an ice bath was considered. An issue was raised, however, over the loss of hydrocarbon molecules to water as it condenses in the ice bath. Instead of this ice bath, a water vapor filter made of 3/8" outer diameter tubing filled with silica gel was used to remove water from the sample gas stream. A Parker-Balston automobile exhaust filter was then placed downstream. This was designed to filter out particulates and condensed water with a 93% gas retention rate at .1 micron. These two devices were used to protect the analyzer from water as well as soot traveling along the sample line. Since the FID setup is not portable, the sampling system had to be designed with this in mind. This was done by using tedlar sample bags as was done in the Schofield study of FIDs.⁶⁹ Tedlar was used as the material for the bags due to its inertness to a wide range of chemicals and its ability to withstand heat. Since the bags could not hold a rigid shape, a gas pump was placed between the filtration/condensation system and the sample bags, which allowed for gas bleeding to the environment at the inlet. This allowed for the flushing of unwanted gas from the sample line up to immediately before the sample bag. A diagram of the sampling system is given in Figure 16.

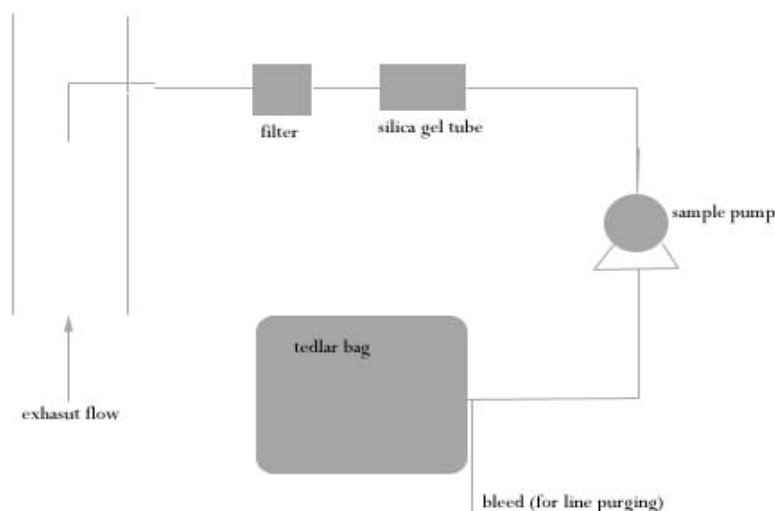


Figure 16: Sampling System

⁶⁸ Schofield, “Problems with Flame Ionization Detectors...”

⁶⁹ Schofield, “Problems with Flame Ionization Detectors...”

The tubing used for the sampling system, fuel, and air lines into the FID were ¼” outer diameter Teflon tubing as seen on Horiba’s own gas analysis bench. The choice of using Teflon tube was supported by Schofield’s observations of stainless steel and Teflon lines minimizing the response time of flame ionization detection. One last issue addressed by his study that is relevant to this FID setup is the use of hydrogen fuel balanced in helium. There is a phenomenon called oxygen interference which can have slight detrimental effects on FID performance. The use of hydrogen fuel balanced with helium has been observed to reduce this effect significantly.⁷⁰ In totality, this equipment was set up with economy and performance in mind. Below is a diagram of the flame ionization detector bench setup used in this study.

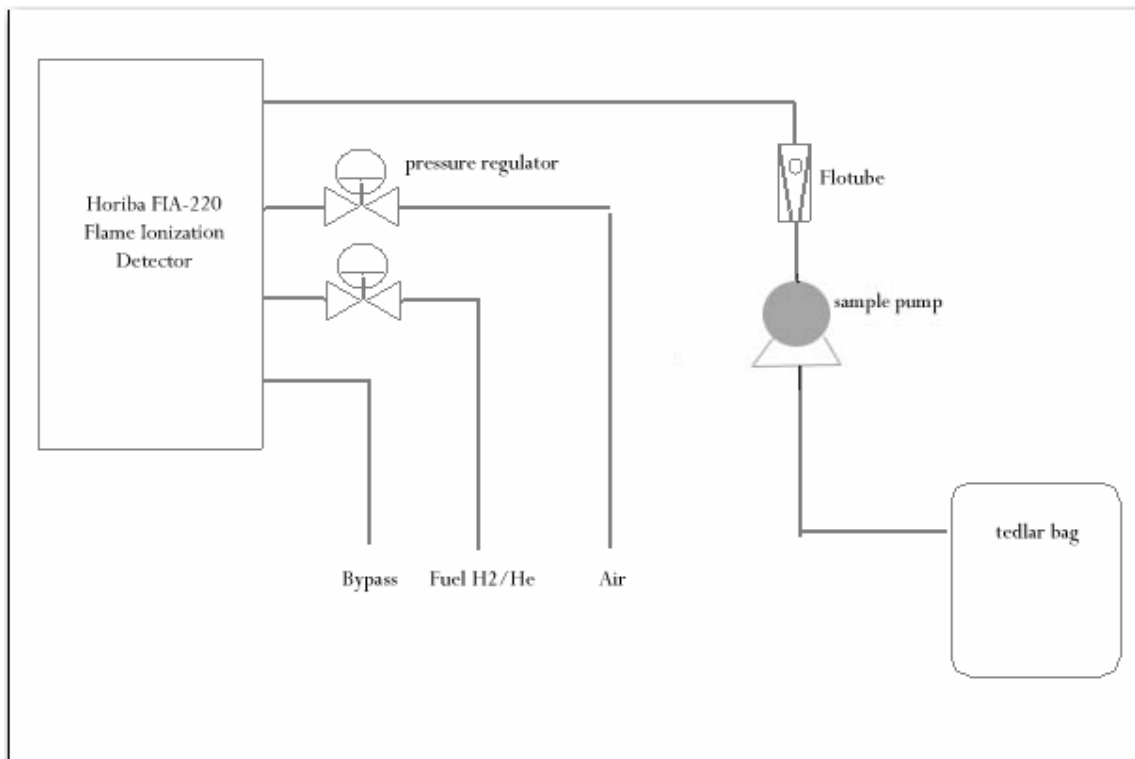


Figure 17 FID Bench Setup

2.4.3 Experimental Procedure for Measuring HC Emissions

Samples for gas hydrocarbon analysis were collected from the vehicle operating in a variety of real-world conditions. These conditions were chosen to gain knowledge of hydrocarbon emissions during common driving as well as under conditions which were predicted to give interesting emissions characteristics. The daily driving routine for many people involves driving on the freeway, so sampling of exhaust gas was performed on a major freeway (I-91) near an urban center (New Haven). A steep hill is also a common driving condition off the freeway. This is also interesting due to the heavier load placed on the engine when accelerating up the hill. RPM data was collected during

⁷⁰ Schofield, “Problems with Flame Ionization Detectors...”

these tests to observe engine speed during the course of each sample collection route. Gas for HC analysis was also collected at idle and during ignition of the vehicle. The idle test was implemented to study hydrocarbon emissions at no load. As for the collection of exhaust emissions during ignition, there was an observed trend of a spike in particulate matter emissions directly after ignition, which would last on the order of seconds. This created interest in studying hydrocarbon emissions in this ignition state.

These procedures for sampling conditions were created with ease of repetition in mind. Since some tests were conducted on public roads and highways with significant urban traffic, it is impossible to recreate exact loads on the car for each test but measures were taken to be as close to exact as possible. For example, routes were planned so that there were no stop lights during its course. The choice of a hot start test instead of a cold ignition test was due to the fact that SVO could not be cold started.

Highway Test: The site for highway testing of HC emissions was I-91 Northbound between the Trumbull street onramp and exit 11. This route was chosen as a suitable route for its lack of steep grades or tight turns as well as its frequent use. I-91's role in Connecticut's intra-state transportation system as a major north-south pathway as well as the route's proximity to the city of New Haven both contribute to the design of this sampling test as it represents a route commonly used by a large population. At the start of the route, cruise control set to 60 miles per hour was activated after entering the freeway from the onramp. The sample line was then purged from the bleed on the sample bag inlet for 45 seconds, ridding the line of any unwanted gases. Exhaust gas was then collected for four minutes at the maximum flow rate provided by the pump.

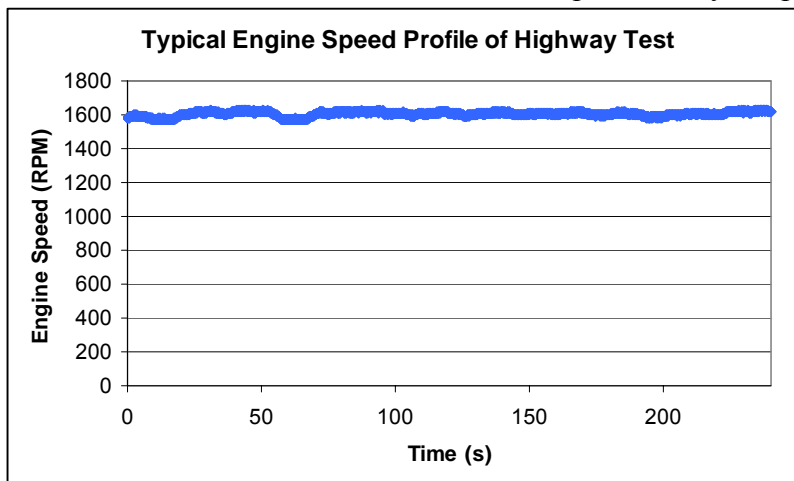


Figure 18 Engine Speed Data for Highway Test

Idle Test: Using the same fill time as the highway test, exhaust gas sampling at idle was performed on the engine after the vehicle had been driven for 10 minutes, allowing for the engine to warm up.

Science Hill Test: In order to observe any interesting HC emission behavior outside of steady engine states, tests were conducted with acceleration and deceleration

incorporated into the route. The route chosen was the stretch of Science Hill starting from the stoplight at the intersection of Prospect St. and Sachem St. to the stoplight at Prospect St. and Edwards St. The sample line was purged for approximately 45 seconds while the car was driven up to the first stop light. The car started from a full stop at this light and accelerated until it reached 40 miles per hour, after which it was held at constant speed until the next stop light. Here the car came to a full stop for 30 seconds. This route lasted approximately 60 seconds total.

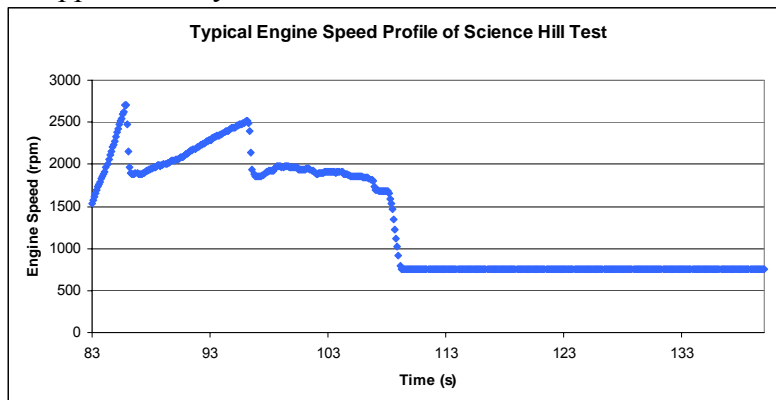


Figure 19 RPM profile of Science Hill Test

Hot Start Test: Sample collection began after the car had been driven for 10 minutes like the idle test. The car was turned off for one minute while the bag was being purged. The bag was then filled for seven ignition cycles consisting of an engine off stage of 5 seconds and an ignition/engine-on stage of 15 seconds. After the seventh cycle, the bag was allowed to fill an extra five seconds for a total of two minutes and 5 seconds. In order to observe hydrocarbon emissions in idle after this series of ignitions, an idle bag was collected one minute after the end of the hot start bag filling.

Procedure for FID calibration and warm-up:

The steps for the calibration and warm-up of the flame ionization detector as outlined in its instruction manual were followed to ensure accurate readings. The zero gas used to zero the machine was nitrogen and the gas used to calibrate the span of the analyzer was propane of a known concentration balanced with zero gas.

Procedure for sample analysis with FID:

Once the bags were collected, they were analyzed using the flame ionization detector. Prior to using this device, the calibration and warm-up procedures were followed to ensure optimum performance from the FID. With the FID primed, a sample bag filled with nitrogen zero air was attached to the sample line. The sample pump was

turned on and the nitrogen air was allowed to purge the sample line for at least one minute.

With the bench now ready for HC analysis, a tedlar bag containing the analysis specimen was attached to the sample line. The sample pump was then turned on to flow the gas being studied into the analyzer. The response time, measured as the time between the start of the sample pump to the time when the FID reading reaches a steady state on the order of 0.1 ppm was approximately 15 seconds. FID readings were thus taken at 15 seconds after the introduction of the sample for all samples to maintain procedural consistency.

2.4.4 Observations of HC Emissions

Repeatability of these tests was demonstrated by taking multiple data sets for many of the tests. The primary baseline test was done with diesel at idle state. Test numbers 22 through 28 were done on the same day so as to have similar ambient variables such as humidity which might affect data. The highest deviation seen in this baseline data set was 5.9% from the mean. This can be attributed to the engine which does not run in the same exact state all of the time as well as other variables such as ambient climate conditions.

Multiple readings were also taken from the same sample bag to calculate procedural and instrumental uncertainty. This uncertainty with this baseline data was found to be on the order of one hundredth of a part per million concentration.

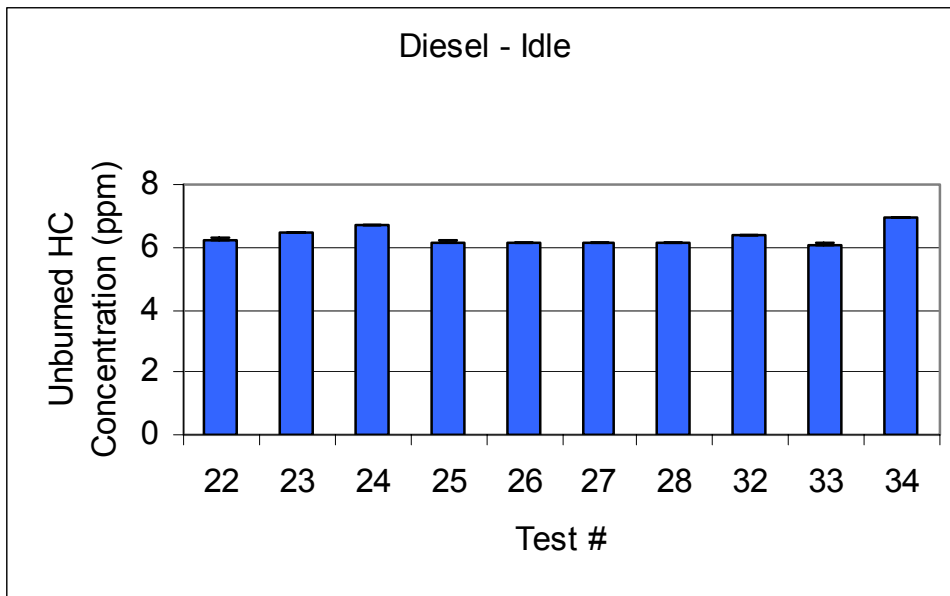


Figure 20 Unburned hydrocarbon emissions from diesel in idle

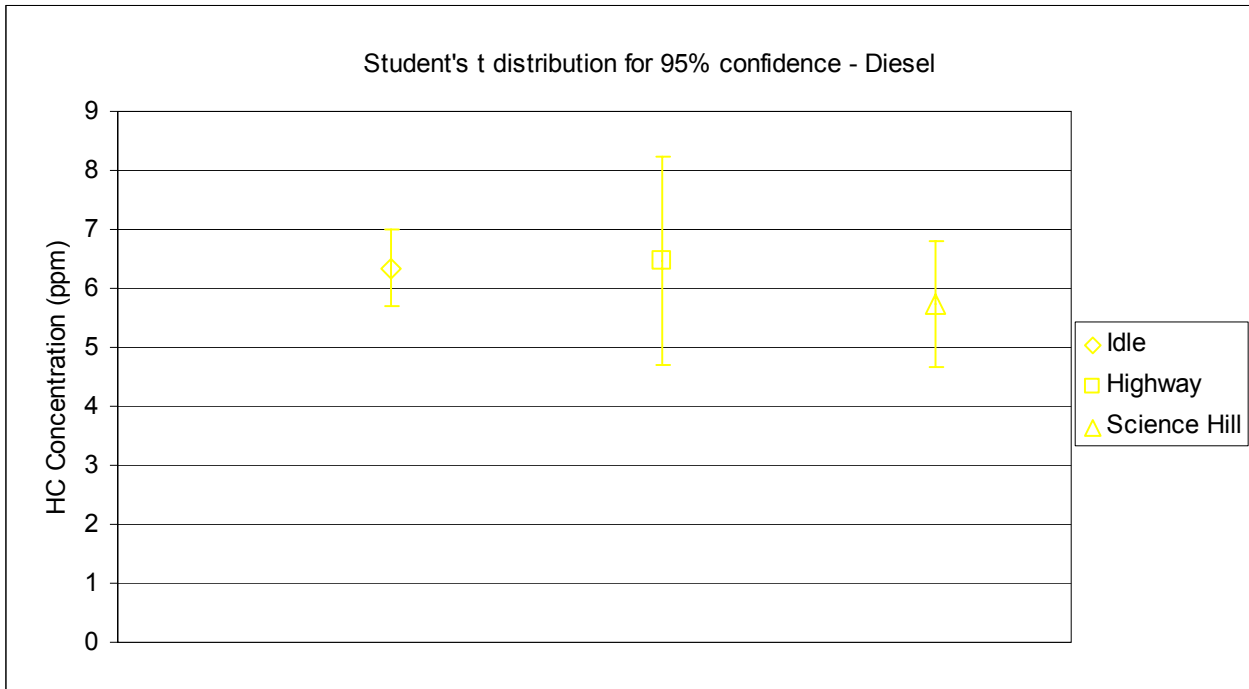


Figure 21 Diesel Fuel Test Comparison

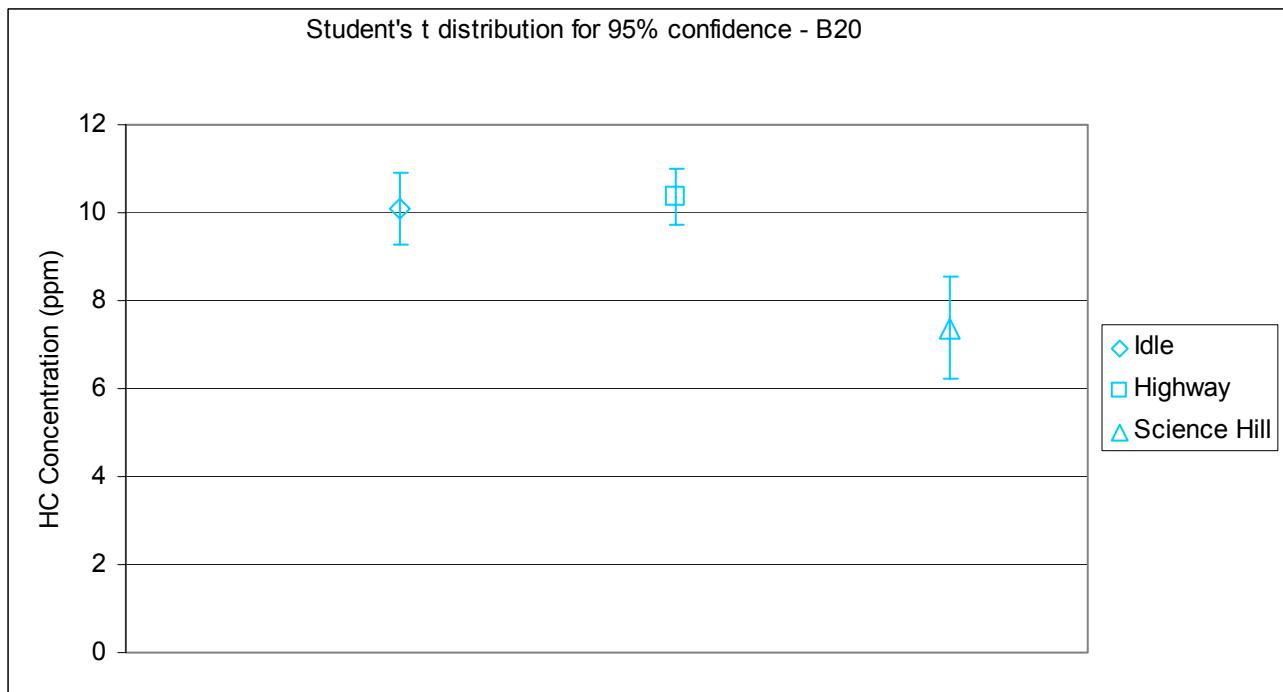


Figure 22 B20 Fuel Test Comparison

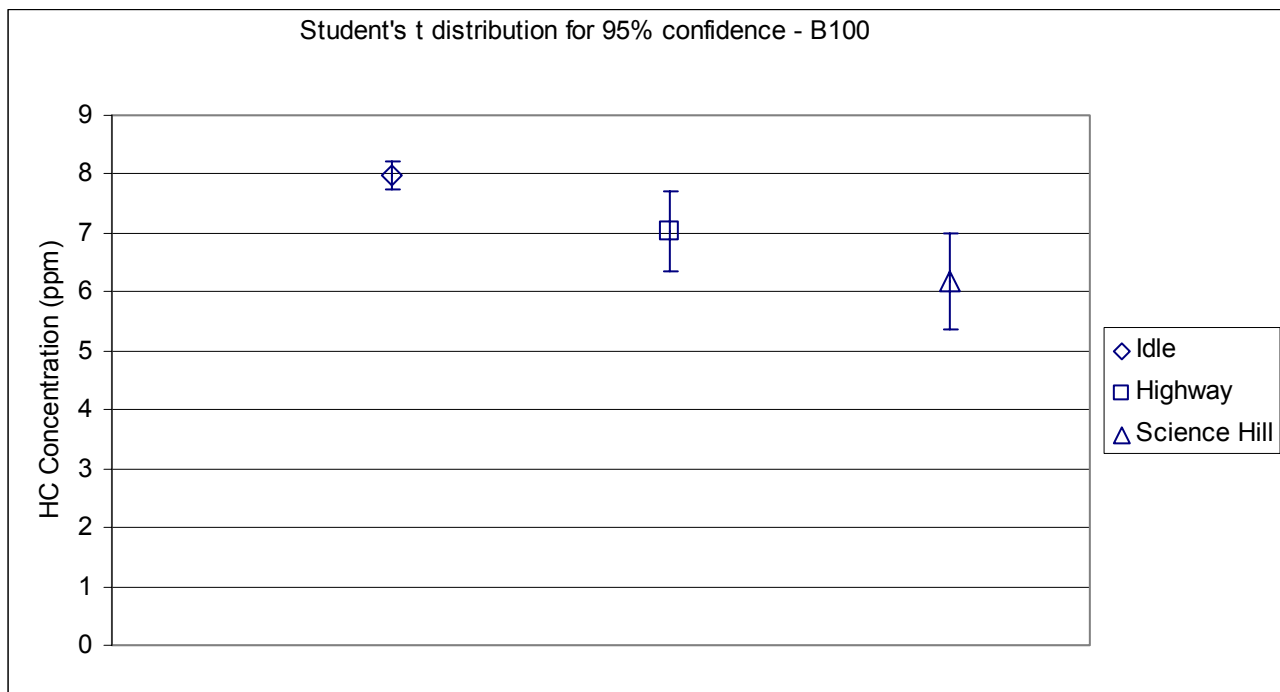


Figure 23 B100 Fuel Test Comparison

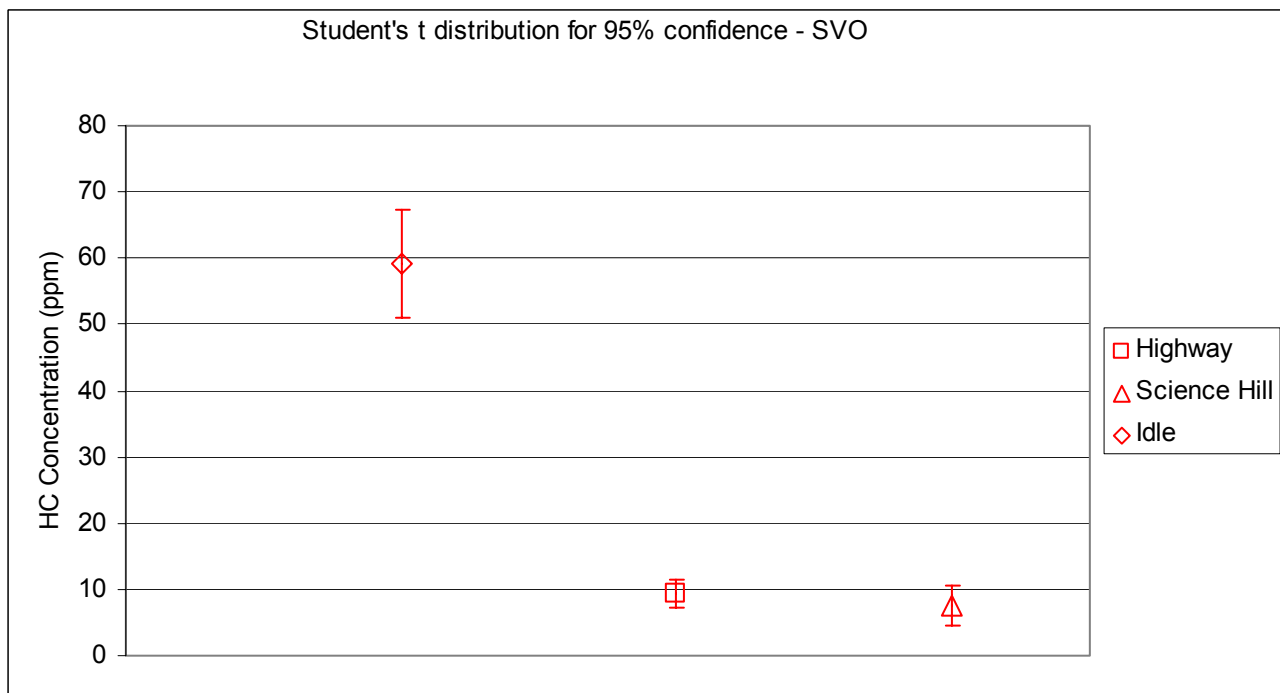


Figure 24 SVO Fuel Test Comparison

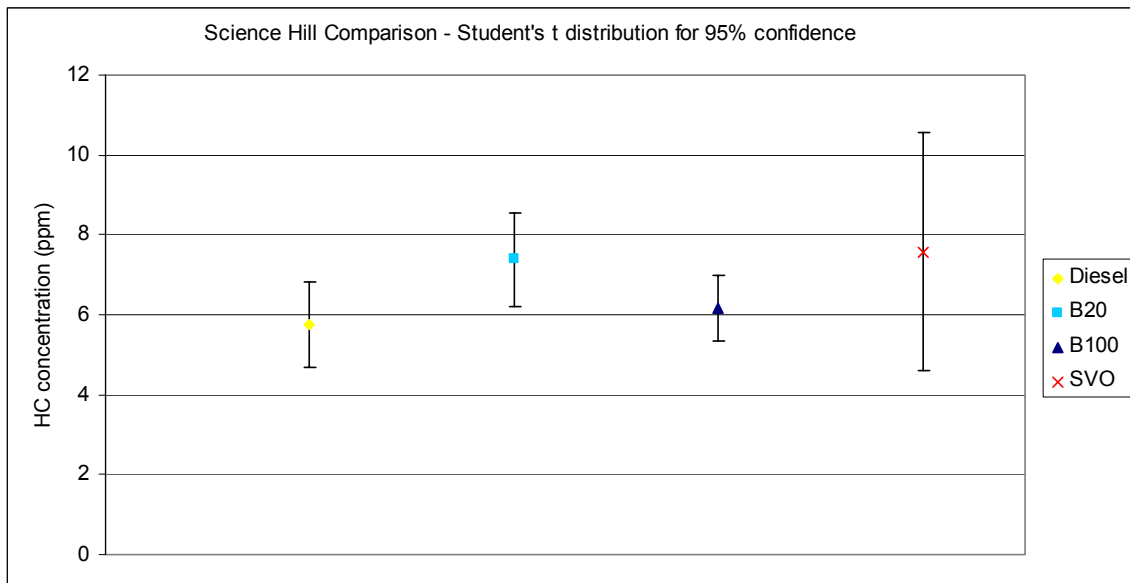


Figure 25 Science Hill Test Comparison

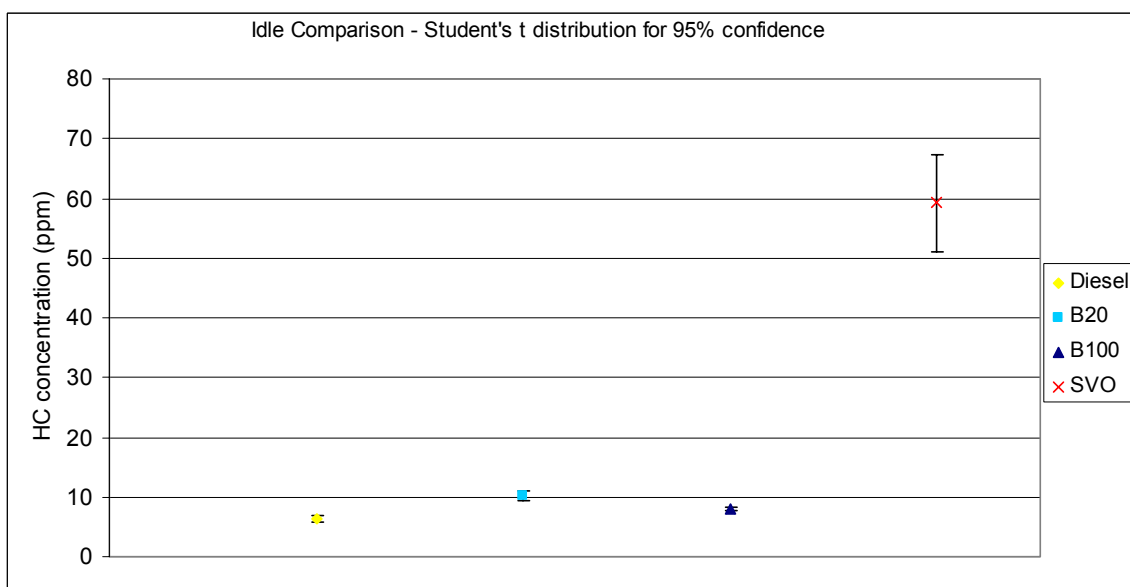


Figure 26 Idle Test Comparison

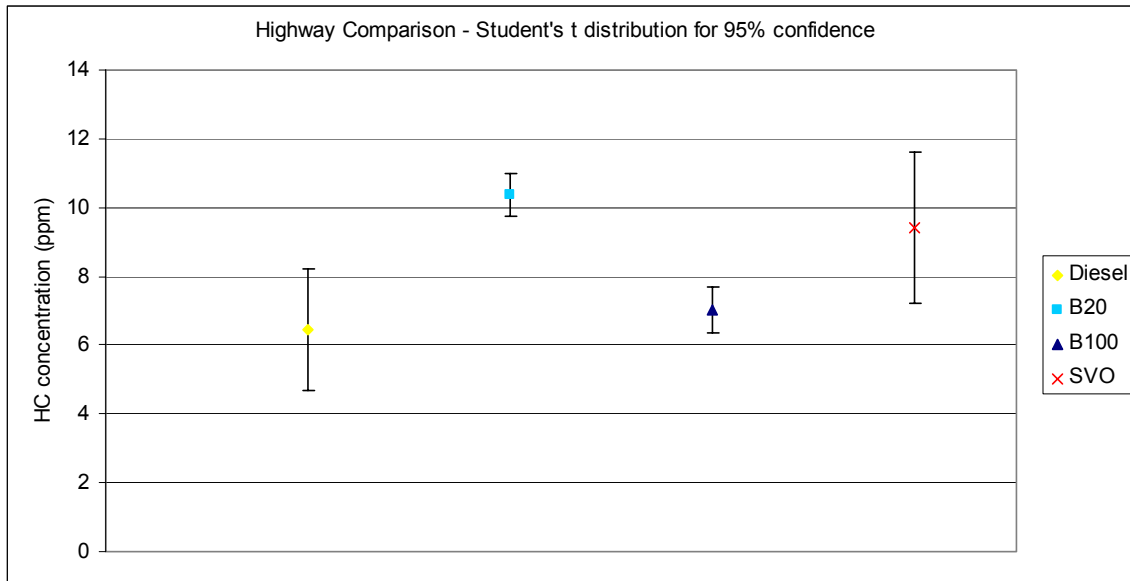


Figure 27 Highway Test Comparison

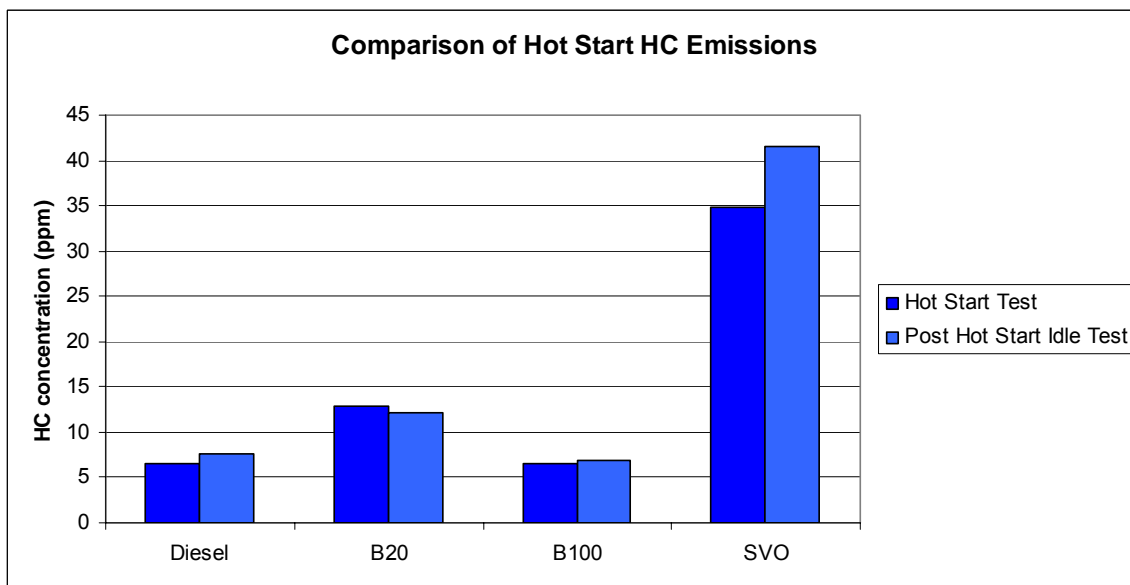


Figure 28 Hot Start Test Comparison

Some trends can be gathered from this data. First, with the exception of SVO, all of these concentrations seem very low. The highest values gathered from tests other than the SVO idle runs showed HC concentrations around 10 or 11 ppm. As a comparison, room air in the Yale Center for Combustion Studies was tested to have at least 1 ppm HC content. Idle emissions on straight vegetable oil showed extremely high HC content compared to all other tests.

An overall trend that can be seen from comparing data for each fuel is that the Science Hill tests seemed to show the lowest hydrocarbon emissions in all of these data sets. It is important to note, however, that this cannot be said with significant statistical confidence for the diesel. The diesel data manifested this trend the weakest. The SVO

also did not show significant drop in HC emissions from the highway test to the Science Hill test. Another trend of the idle tests having higher values is not significant in the diesel and B20, yet this trend becomes visibly prominent in the B100 and SVO.

When comparing different fuels for each test, a visible trend in the idle, highway and Science Hill data is that diesel and B100 sets have similar emission values which are lower than those of the B20 and SVO. This catches the eye because the mean values of all of the data could be characterized by this trend; however, a closer look at the student's t distributions shows that it cannot be said to exist with 95% confidence. A trend that is statistically significant can be found in the idle data – the SVO emissions were much higher than the emissions from the other fuels. The hot start test data saw the same trend.

An interesting note on the hot start results is that there was only slight relative change between the hot start test and the idle test which came a minute afterward. There seems to be no new trend seen in this data.

2.4.5 Discussion of Observations for HC Emissions

The composition of unburned and partially oxidized hydrocarbons in diesel exhaust is a complex mixture which has a large molecular size variation. With this statement arises an issue with the experimental procedure of this study. The use of an unheated FID results in the loss of some higher molecular weight hydrocarbons which condense out of the vapor stream.⁷¹ Other studies have shown HC emission concentrations ranging from tens of ppm to hundreds of ppm.^{72, 73, 74} This could explain why the FID outputs for this entire experiment seem rather low comparatively. The HC measurements in this study do not incorporate the heavier hydrocarbons which are condensed out and filtered along with the soot in the sampling system. Studies using heated flame ionization detectors which can heat samples to over 400 degrees F show over 10% difference in readings from unheated and heated FIDs.⁷⁵ There is a possibility that this loss of hydrocarbon sensitivity is affecting the trends seen in this data. Therefore, further research of HC emissions using this setup should incorporate a study of the hydrocarbon composition of the exhaust mixtures analyzed. Also, the use of a heated FID to measure HC emissions should be stressed in the future to prevent any loss of HC from the analyzed gas.

When discussing hydrocarbon emissions in the context of the vehicle and its performance, it is important to study what occurs inside the engine in the context of different fuels having different properties. Unburned hydrocarbon emissions depend on the state of the engine, atomization of fuel, and the behavior of the fuel-air mixture in the cylinder.^{76, 77}

⁷¹ Heywood. *Internal Combustion Engine Fundamentals*, p. 620.

⁷² Pokharel et al. "On-Road Remote Sensing of Automobile...".

⁷³ Tsolakis et al. "Exhaust gas assisted reforming of rapeseed methyl ester for..."

⁷⁴ Lee et al. "An Experimental Study on the Atomization..."

⁷⁵ Schofield. "Problems with Flame..."

⁷⁶ Canakci et al. "Comparison of Engine Performance and Emissions..."

⁷⁷ M. Canakci, A. Erdil, and E. Arcaklioglu. "Performance and Exhaust Emissions of a biodiesel engine," *Applied Energy*, Elsevier: 2005. Vol. 83, pp 594-605.

In terms of engine conditions, the idle, Science Hill, and highway tests can be categorized into three engine states. Idle is its own state, representing the lowest extremity of engine load. The Science Hill test represents a heavy load and the highway test represents an operating state somewhere between the other two. For a direct injection diesel engine, idling and light-load states produce higher hydrocarbon emissions than when an engine is under a heavy load.⁷⁸ This would explain higher emissions observed during idle tests.

Overmixing, also known as overleaning, is a major source of HC in various engine states. Studies have shown the effect of this to be most significant at idle and at low-loads.⁷⁹ Overleaning happens when the fuel-air ratio becomes too lean in certain regions of the cylinder. In these realms, there is incomplete combustion, resulting in increased HC emission. The extent of overleaning is strongly associated with ignition delay, as well as with the mixing of air and fuel during this period. Shorter ignition delays can decrease HC emissions. More complete combustion occurs with better atomization and therefore this can also improve HC emissions. An explanation for the pattern that can be seen by comparing the mean HC emissions for each fuel where the diesel data and B100 data are lower than the B20 and SVO data may be a result of a balance of these two factors controlling the magnitude of overleaning. The biodiesel has a higher cetane number and has 10-11 percent oxygen content by weight, the combination of which reduces ignition delay.⁸⁰ However, biodiesel has higher kinematic viscosity and surface tension. The significance of these two properties can be explained in terms of atomization. Atomization performance varies with injection velocity and the Weber number. Higher kinematic viscosity reduces injection velocity of the fuel jet due to increased friction effects. Increased surface tension properties are related to a decrease in Weber numbers. Both lower Weber number and lower injection velocity lead to larger fuel droplets and worse atomization.⁸¹ In order to put this information in the context of the previous observations seen in this study, the lower HC emissions of diesel compared to B20 represents the domination of diesel's superiority in its atomization as well as with the manufacturer's design and optimization of the vehicles performance based around the use of diesel fuel. The lower emissions that arose from using B100 over B20 represents the region where biodiesel's oxygen content and higher cetane number contribute greater to the engine's performance in terms of HC emissions. Furthermore, to explain the significantly higher HC emissions of SVO, one can return to the contribution of poor atomization. The viscosity of SVO is an order of magnitude higher than that of biodiesel.⁸² If typical viscosities of commercial automobile diesel and soy based biodiesel are 2.83 and 4.27 respectively (nowhere near an order of magnitude difference), using SVO would give a much larger performance loss due to much worse atomization. The most pronounced differences between the hydrocarbon emissions performances of the fuels occur at the lowest load state (idle). This supports previous observation that

⁷⁸ Heywood. *Internal Combustion Engine Fundamentals*. pp. 622.

⁷⁹ Stephen Carter, J. Gary Hawley, John Slowley. "Initial Development of a Predictive Hydrocarbon Emission Model for a DI Diesel Engine," University of Bath, Indiana, IEEE, 1996.

⁸⁰ Heywood. *Internal Combustion Engine Fundamentals*. pp. 623.

⁸¹ Lee et al. "An Experimental Study on the Atomization..."

⁸² G Knothe, "Dependence of Biodiesel fuel properties on the structure of fatty acid alkyl esters" *Fuel Processing Technology*, Elsevier: 2005, Vol. 86, pp 1059-1070.

overleaning is a dominant contributor to HC emissions in light load operation. This is the result of longer ignition delay associated with the idle state.⁸³

The significance of the hot-start tests is less clear. The differences in the hot start and post-hot start idle numbers are affected by the 35 seconds of gas sampling time which were spent while the bag was filling when the engine was off. Since there were no significant observed differences between the hot-start and idle tests for the same fuels, one can conclude that the mechanisms which contribute to the majority of particulate formation at ignition differ from the mechanisms which control the emissions of unburned hydrocarbons.

2.4.6 Conclusions on HC Emissions

The fact remains that there is some inevitable loss of heavy hydrocarbon due to the ambient temperature at which the current FID bench operates. To correct this problem, a heated flame ionization detector should be implemented. Although this injects some amount of uncertainty over the entire HC study in terms of studying total unburned hydrocarbon emissions, it cannot be neglected that the data that was collected did provide useful contexts for studying the effects of the use of different fuels on unburned hydrocarbon emissions.

Trends seen in the data could be supported by the contribution of overleaning in the engine to HC emissions, which is most noticeable in idle. The behavior of HC emissions at idle was significantly pronounced from the rest of the data.

The forced remote sampling of exhaust gas due to the use of the vehicle as a testing apparatus allowed only for integrated measurements of HC emissions at various states. With the use of a more controlled combustion environment such as a diesel generator set in conjunction with a dynamometer, quantitatively significant conclusions about the effect of different engine states on HC emissions can be drawn through instantaneous measurement of exhaust.

By having a more ideal laboratory setup, variations in the data of this study which were most likely due to variables beyond control, such as weather, would be reduced. The direct optimization of and experimentation with the diesel generator would result in tightly controlled observations of the phenomena which occur inside the engine and thus would lead to better understanding of the mechanics of hydrocarbon emissions.

⁸³ Carter et al, "Initial Development of a Predictive Hydrocarbon..."

3. PROJECT CONCLUSIONS

This project was a study in the feasibility of the use of a diesel vehicle for the testing of biofuel performance in the realm of exhaust emissions. By benchmarking the emissions of the vehicle running on biofuels against those of well-researched petroleum-based diesel fuel, the project was able to draw some conclusions about the use of biofuels which could be compared with current research on the subject.

The merits of the project lay in its success in establishing a base knowledge about the effect of biofuel use in vehicular emissions with the use of limited equipment and resources. An indirect consequence of this was to spark more undergraduate interest in undertaking research in the field of sustainable fuel use.

Much of the uncertainty that was associated with data in this project was a result of the use of a vehicle to perform on-road tests in an urban populated area. There are too many uncontrolled variables associated with this study's procedure, and thus, the next step in Yale's undergraduate biofuels research should be to expend its resources on creating a more controlled experimental environment. This would exponentially increase the potential for precise research, and it would also foster the implementation of newer, forward-thinking concepts in the field of sustainable energy.

Acknowledgements

The Yale Biofuels team would like to acknowledge the following people who have kindly supported us with their wisdom and generosity:

Alessandro Gomez

Wei Wei Deng

Bruno Coriton

Glenn Weston-Murphy

Ed Jackson

Nick Bernardo

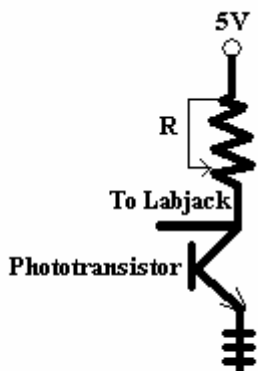
Gus Kellogg, Greenleaf Biodiesel

Jon Van Gerpen

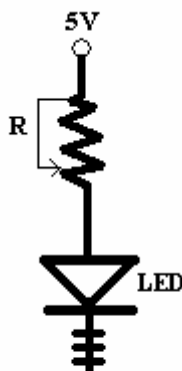
Doug Miller, Horiba USA

The Yale Engineering Design Team

Appendix A: Relevant Information for PM Section

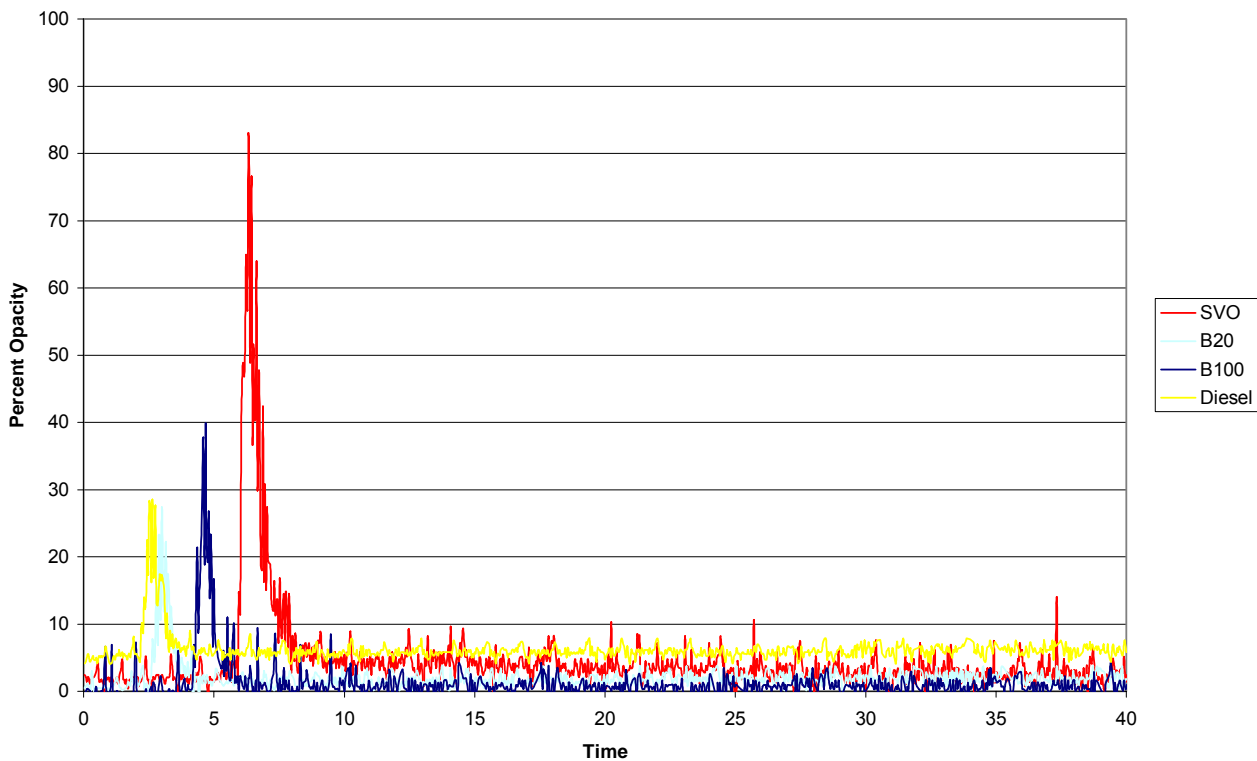


Light Detector Circuit Diagram

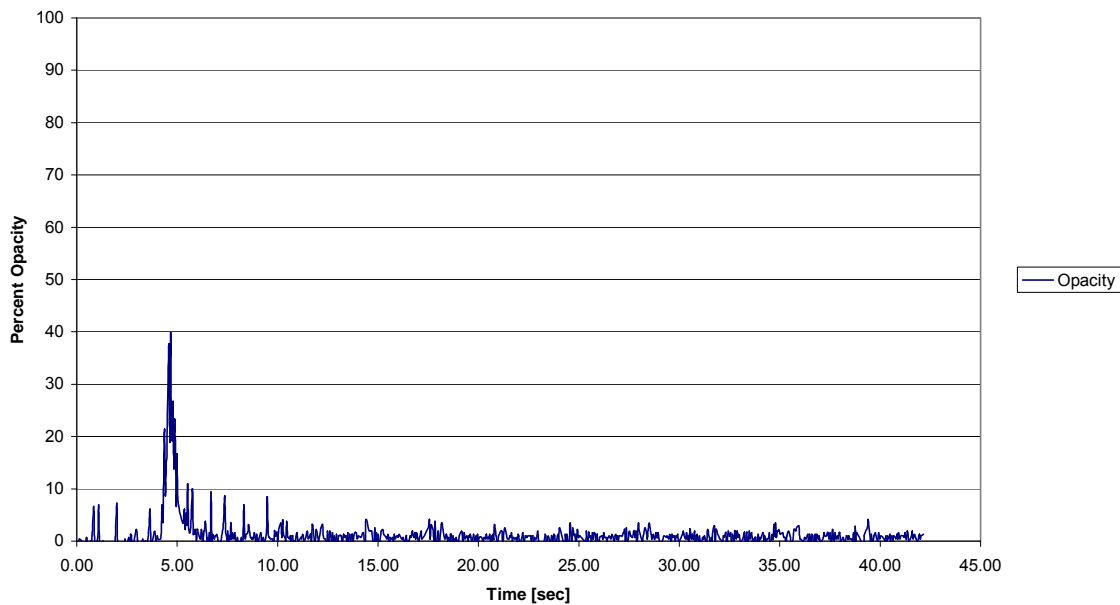


LED Circuit Diagram

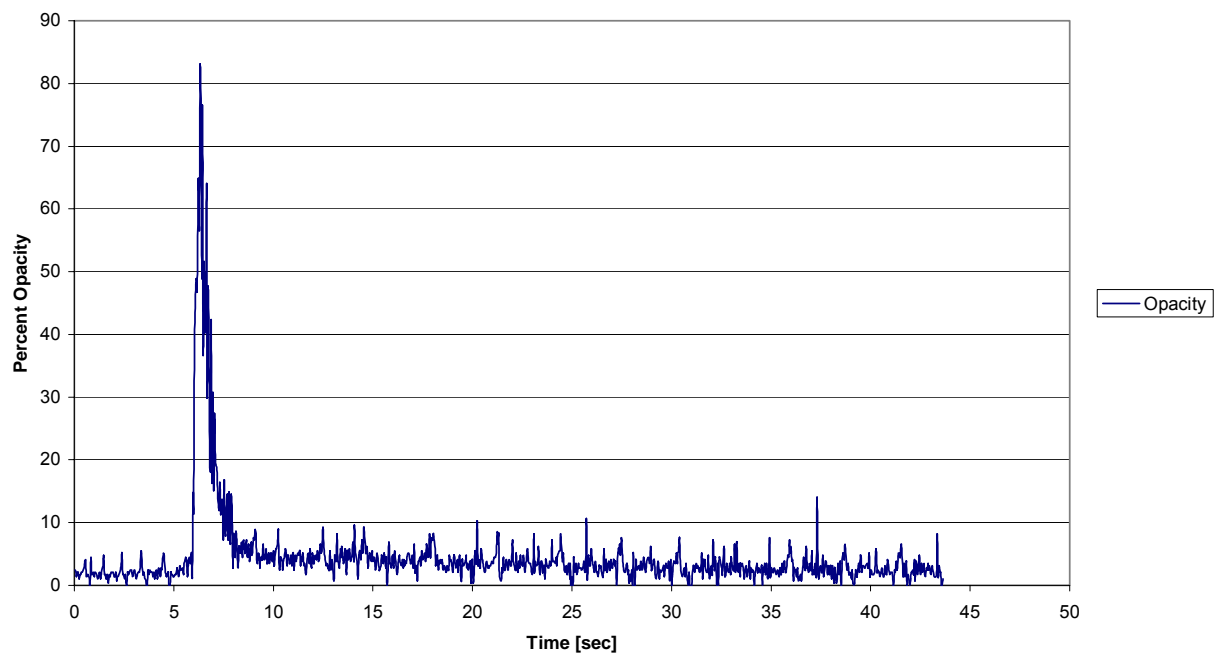
Hot Starts



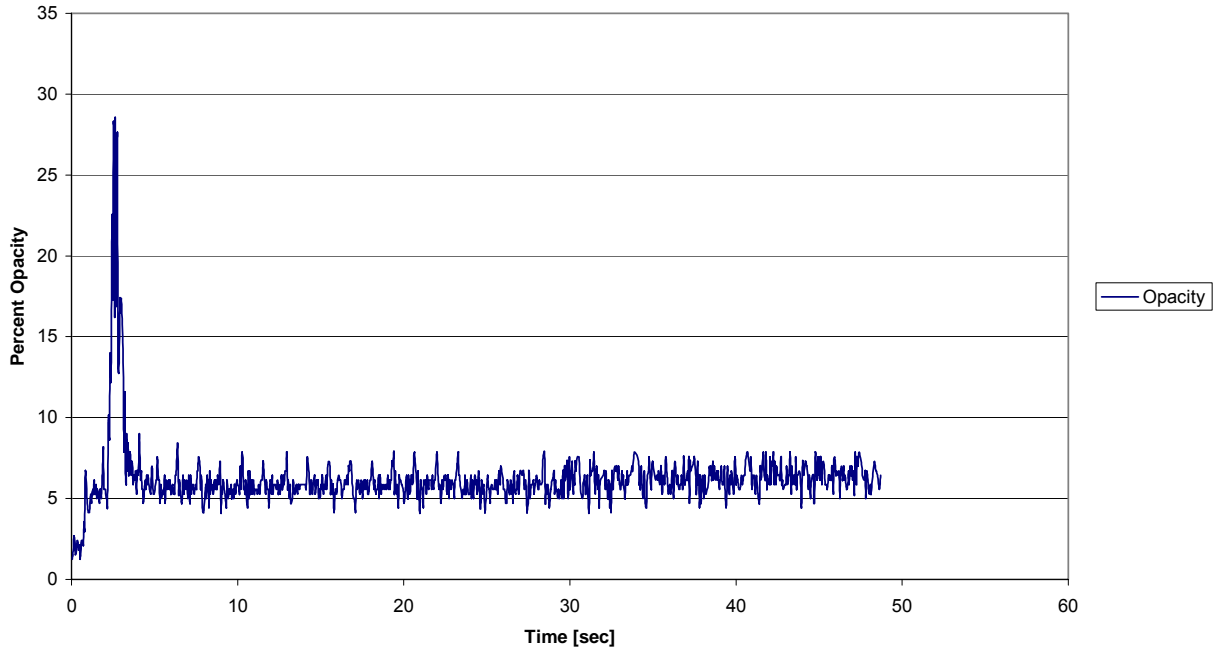
Opacity Hot Start B100



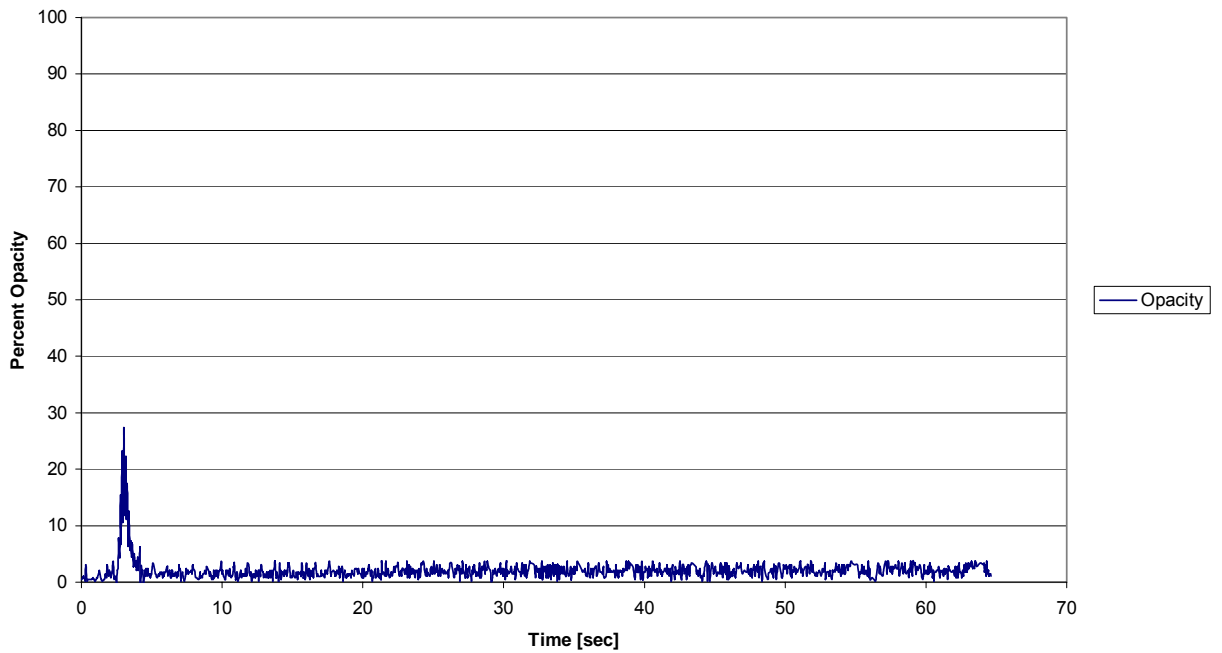
Opacity - Hot Start Veg Oil



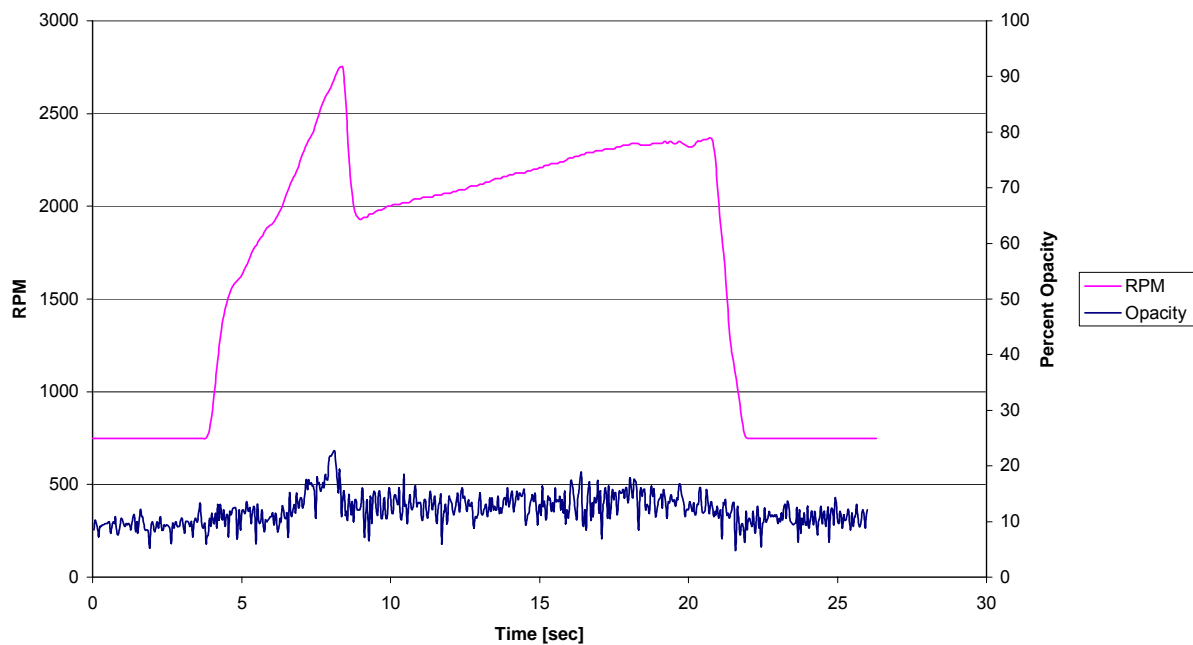
Opacity - Hot Start Diesel



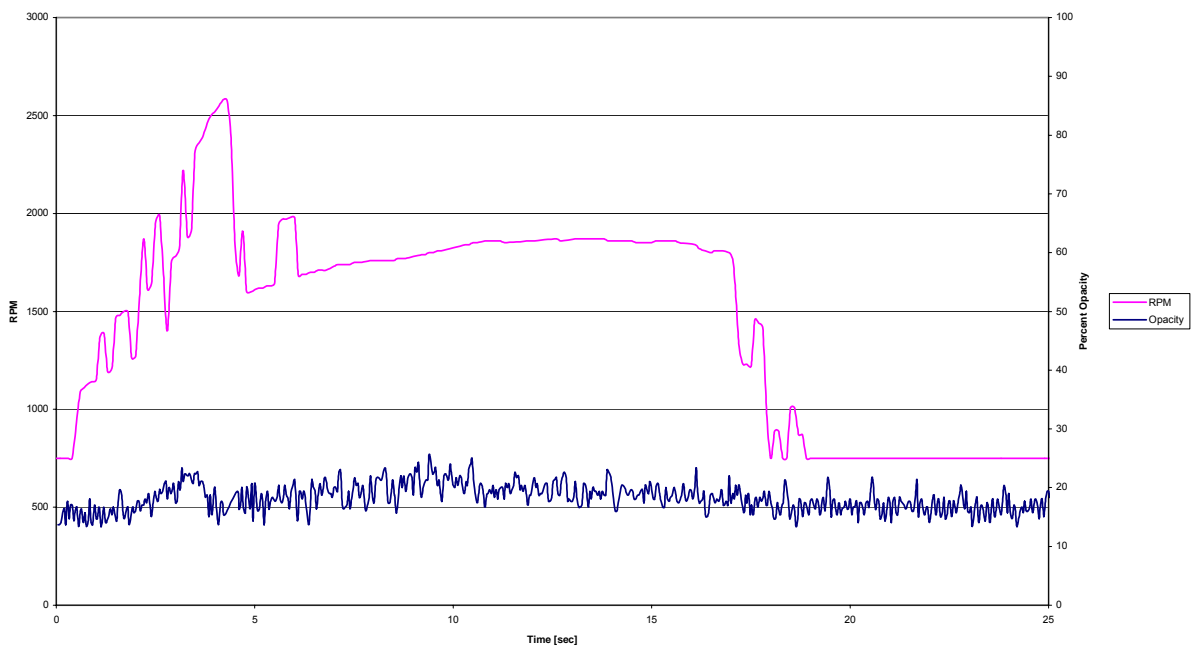
Opacity - Hot Start B20



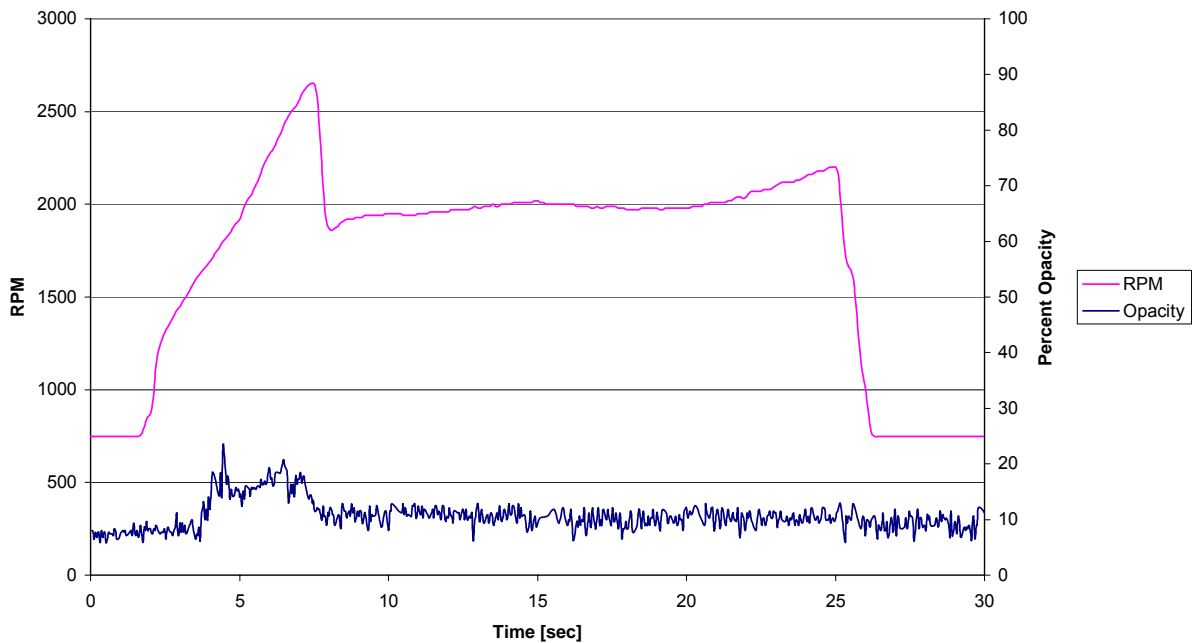
Canner Hill Diesel



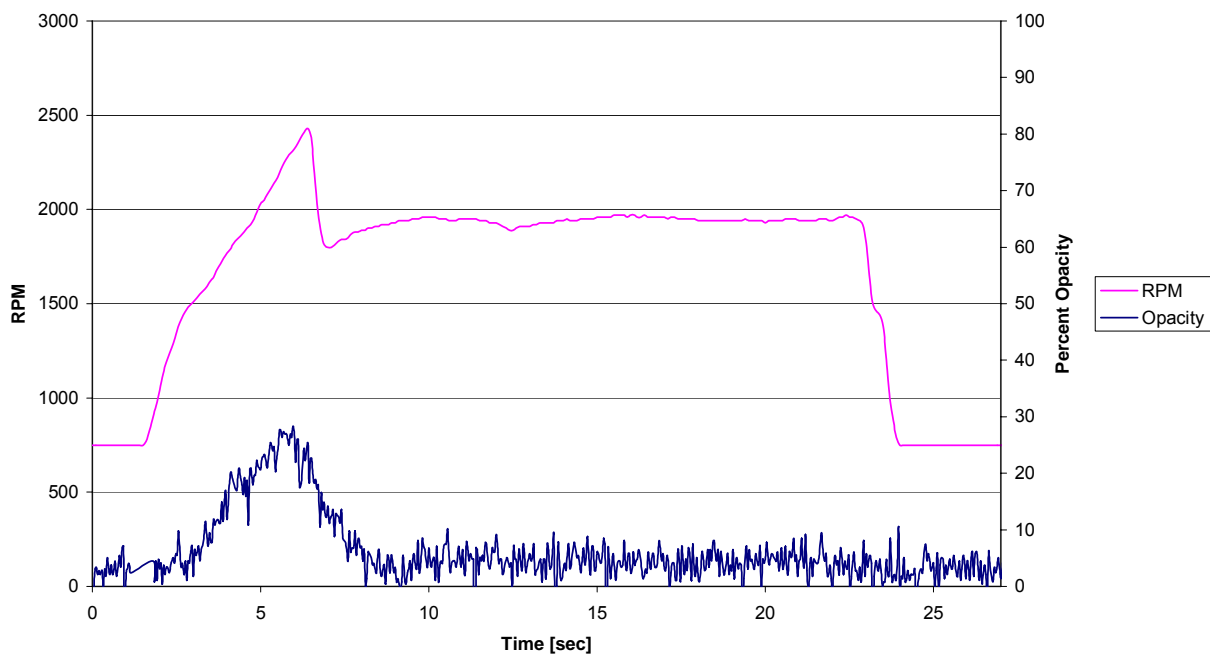
Canner Hill B20



Canner Hill B 100



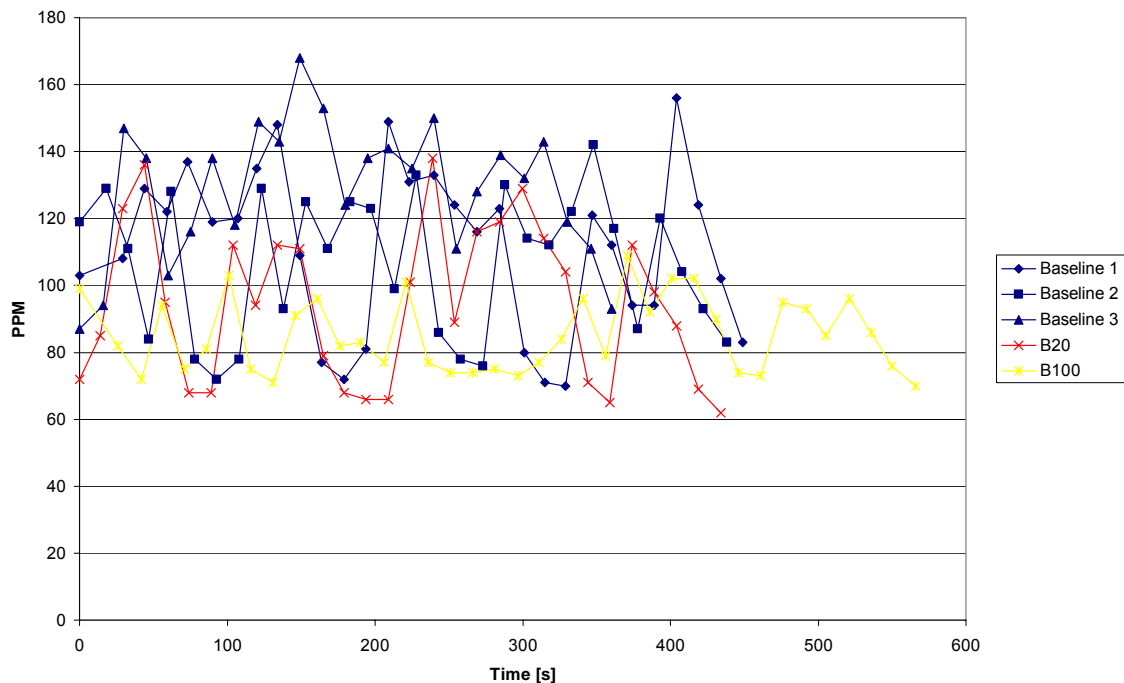
Canner Vegetable Oil



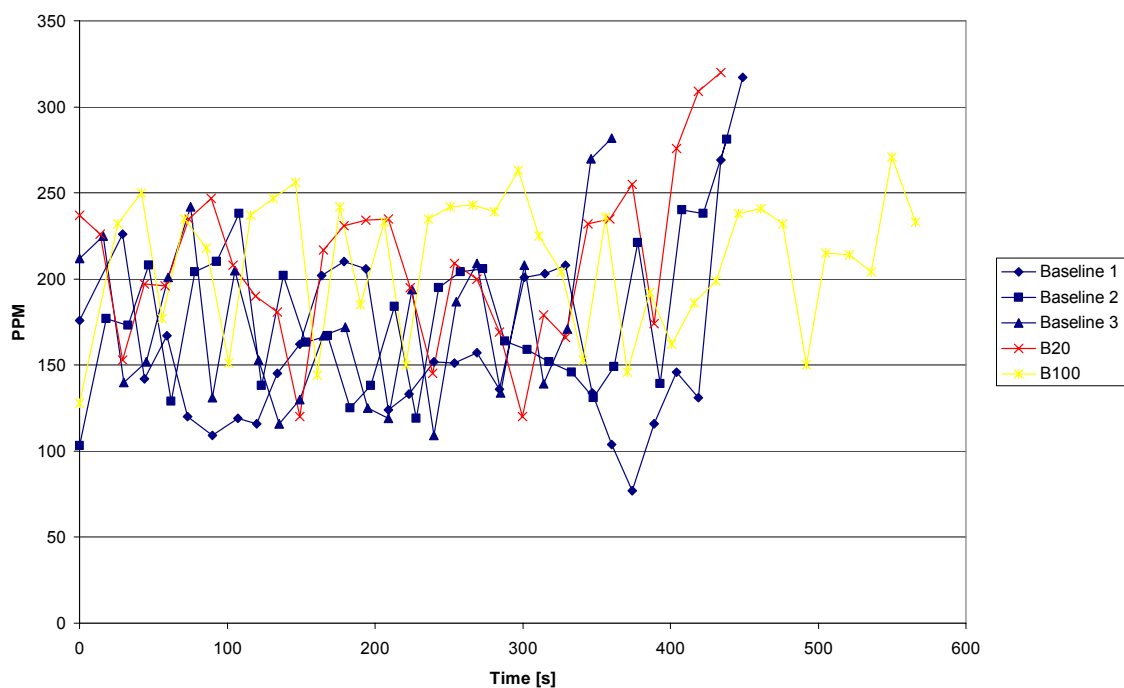
	Hot start peak opacity	σ	Soot Density (mg/m ³)	σ	Hot start idle opacity	σ	Soot Density (mg/m ³)	σ
Diesel	28.55	1.43	763	38	6.38	0.32	150	7.48
B20	27.16	1.09	719	36	2.15	0.09	49	2.32
B100	39.86	1.59	1154	58	0.797	0.04	18	0.73
Vegetable Oil	82.67	3.89	3978	199	2.67	0.11	61	3.07
	Idle 1 opacity				Idle 2 opacity			
Diesel	6.58	0.33	154	7.7	7.75	0.31	183	8.6
B20	2.3376	0.09	54	2.7	2.9	0.14	67	2.67
B100	1.47	0.07	34	1.7	1.88	0.08	43	2.15
Vegetable Oil	1.49		34	1.7	1.45	0.07	33	1.56
	Prospect Load opacity				Prospect peak opacity			
Diesel	7.85	0.37	186	9.3	16.67	0.83	414	16.6
B20	12.7	0.64	308	15	20.36	0.96	517	25.8
B100	5.51	0.22	129	6.4	18.6	0.93	467	23.4
Vegetable Oil	1.74	0.09	40	2	27.94	1.12	744	37.2
	Canner Load opacity				Canner Peak opacity			
Diesel	15.76	0.74	389	16	22.73	1.14	585	27.5
B20	17.37	0.87	433		23.34	1.1	603	30.2
B100	10.25	0.51	245	12	18.48	0.74	464	23.2
Vegetable Oil	4.78	0.24	111	5.2	28.35	1.42	757	30.3
	Edwards Load opacity				Edwards Peak opacity			
Diesel	9.39	0.47	224	11	17.58	0.83	439	21.9
B20	5.76	0.29	135	5.4	11.09	0.55	267	10.7
B100	7.1	0.36	167	7.9	20.38	0.82	517	25.9
Vegetable Oil	3.09	0.15	71	3.6	43.17	2.03	1282	64.1
	Highway 1 rpm 1600 opacity				Highway 2 opacity			
Diesel	11.624	0.55	280	14	11.92	0.6	288	11.5
B20	4.136	0.29	96	3.8	6.91	0.28	162	8.12
B100	0.96	0.05	22	1.1	0.77	0.04	18	0.88
Vegetable Oil	0.136	0.01	3	0.1	1.59	0.08	36	1.45

Appendix B: Relative Information for CO and NO_x Emissions

Fuel Comparison - CO - City

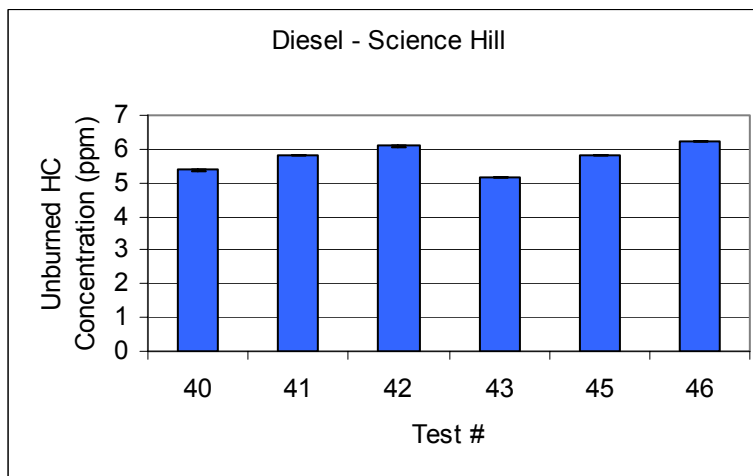
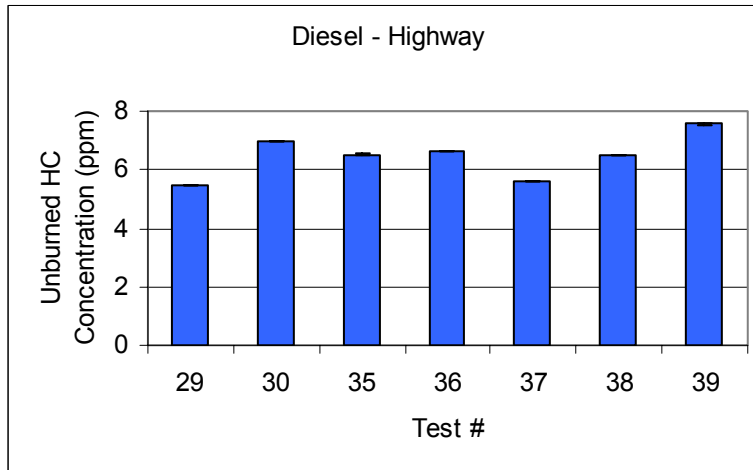
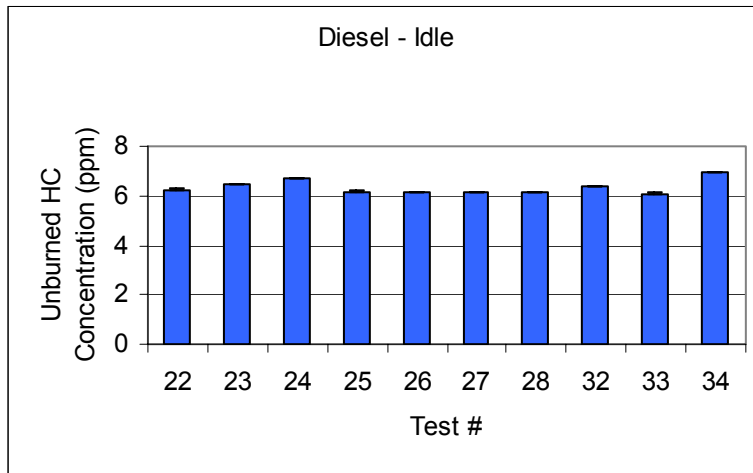


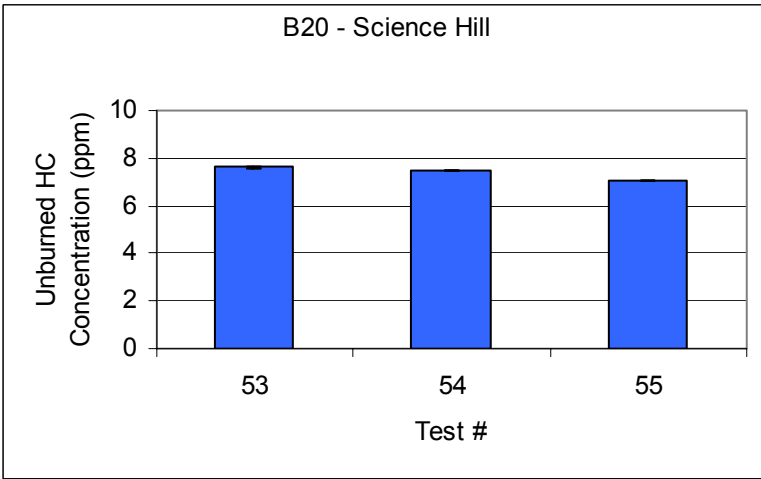
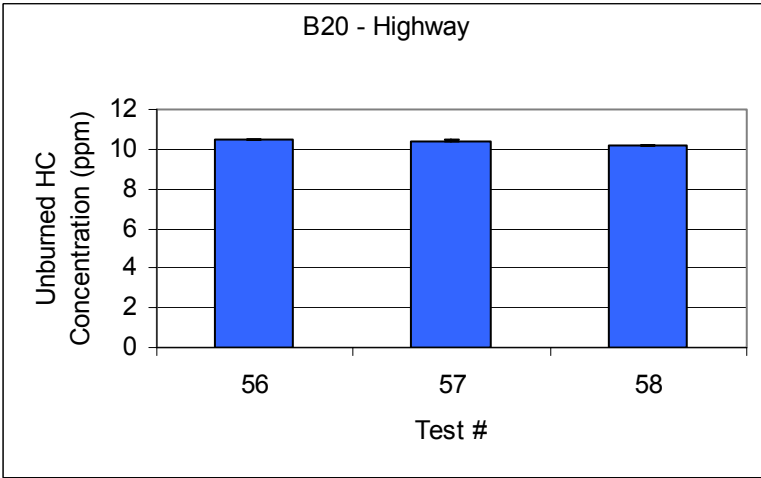
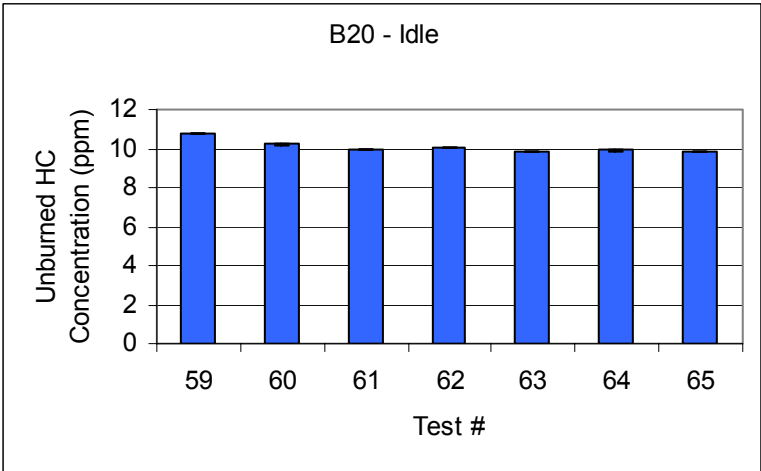
Fuel Comparison - NO_x - City

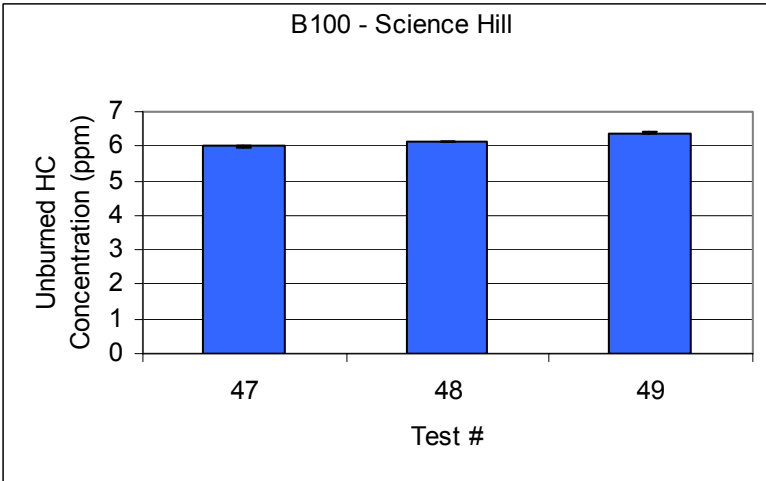
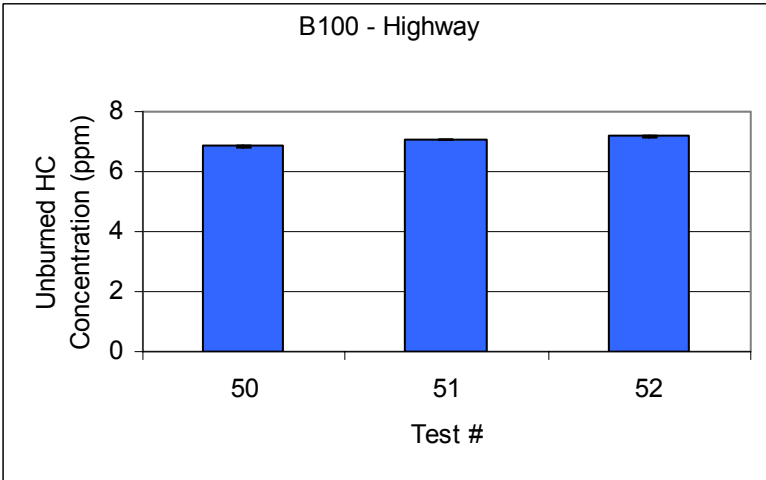
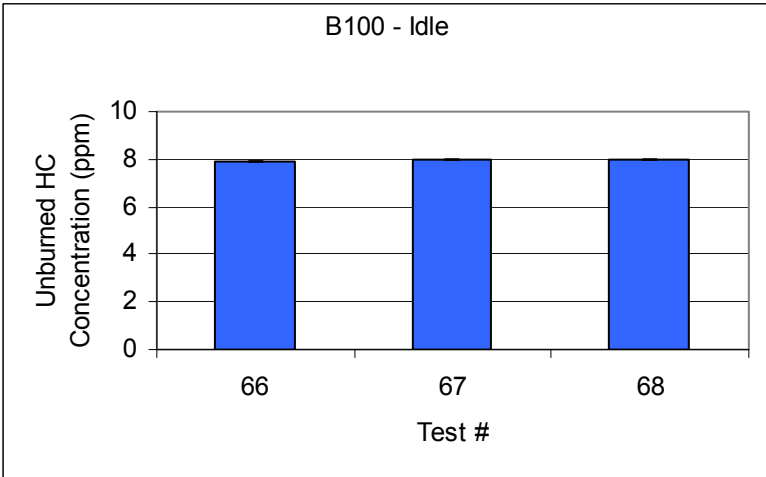


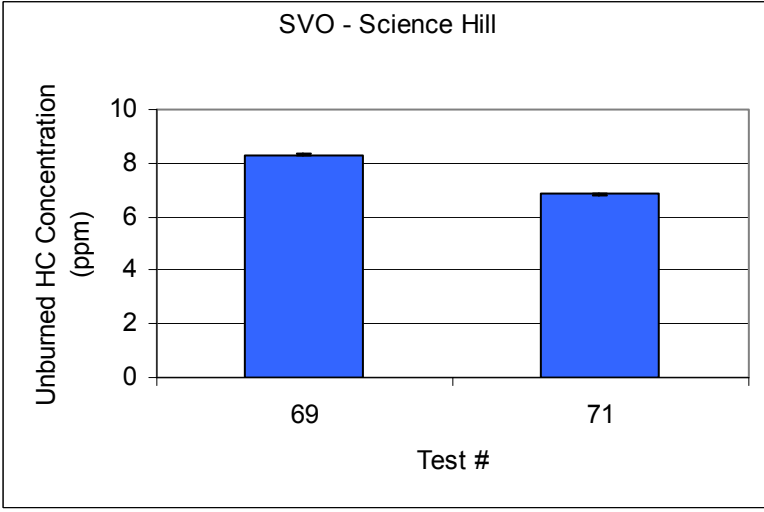
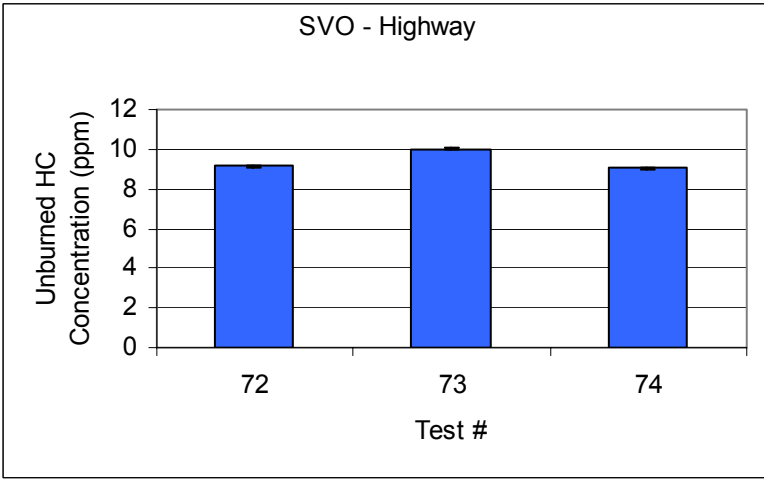
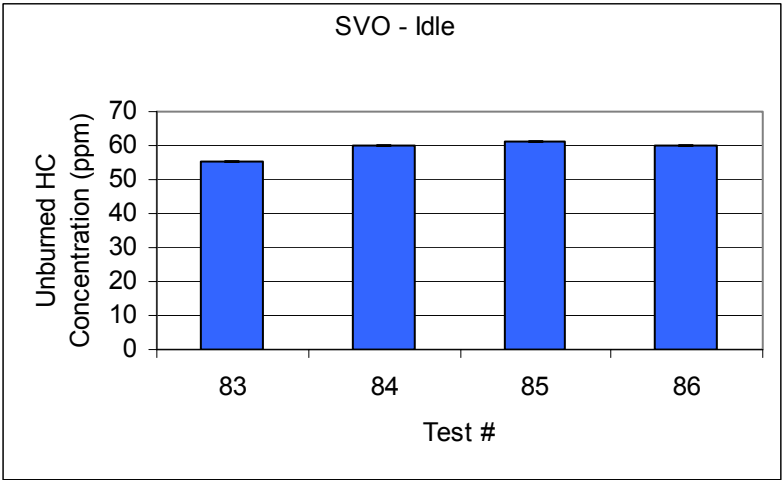
Appendix C: Relative Information for HC Emissions

Raw data

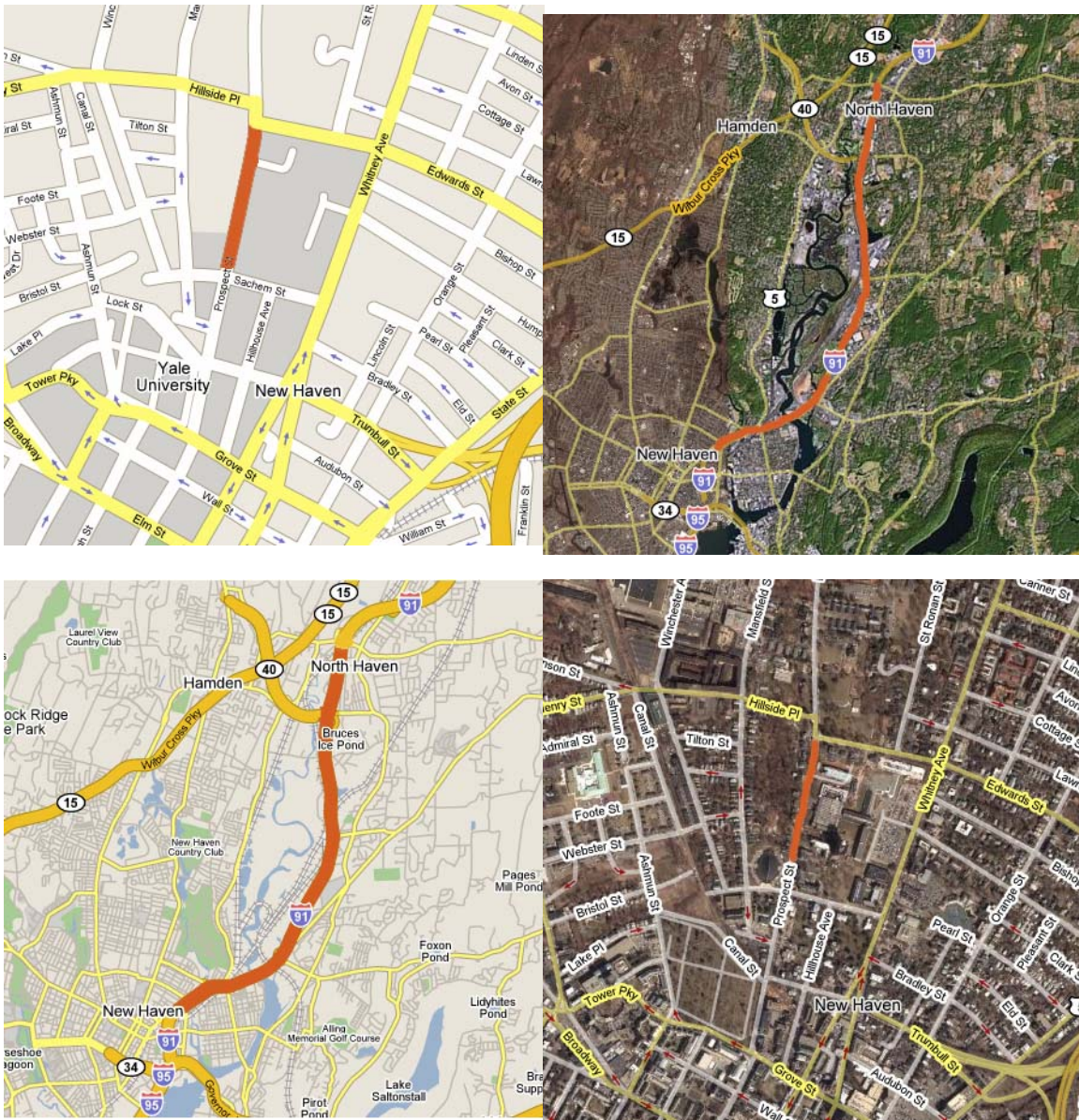








Road Test Routes



Appendix D: Electroacoustical Estimate for Dampening Chamber Size

Because the Bacharach PCA was not designed to handle the exhaust pulses occurring at the tailpipe of a vehicle, a dampening chamber was proposed and designed. In order to obtain a rough estimate of appropriate volume for the chamber, as well as to understand design variables that can help buffer the flow, a simple analogy between fluid dynamics and electric circuits was created. In this electroacoustical analysis, gas flows correspond to currents, volumes become capacitors, pressure relates to voltage, and flow resistance (which yields pressure drops) is represented by resistors.⁸⁴

Since we were interested in dampening the pulses of the exhaust, we sought to find an acoustical equivalent to an RC circuit. If we could design a chamber with a time constant τ sufficiently larger than the characteristic time of the pulses, we would be able to buffer them out. According to Beranek, resistance can be represented by a pressure drop over a corresponding volumetric flow rate,

$$R = \frac{\Delta p}{\dot{V}} \quad [\text{kg}/(\text{s} \cdot \text{m}^4)] \quad (\text{Eq. 1})$$

while the capacitance can be approximated by

$$C \approx \frac{V}{\gamma P_0} \quad [\text{m}^4 \text{s}^2 / \text{kg}] \quad (\text{Eq. 2})^{85}$$

Utilizing the fact that $\tau = RC$ and combining the equations, it is easy to see that

$$V = \frac{\dot{V} \gamma P_0}{\Delta p} \tau \quad [\text{m}^3] \quad (\text{Eq. 3})$$

γ can be taken to be 1.4, P_0 is given by atmospheric pressure, and we can design for a value of $\tau = 10t$, where t is the time between every exhaust pulse. At an RPM of 1600, and because there is one exhaust stroke for every two cycles of the engine, we come up with a value of $1600 \text{ RPM} \cdot 1 \text{ min}/60 \text{ s} \cdot 1 \text{ exhaust}/2 \text{ rotations} = 13.3 \text{ exhausts/second}$. This gives a t -value of .075 s, and $\tau = .75 \text{ s}$.

The flow rate can be estimated by using a reasonable assumption for the exhaust velocity at the tailpipe multiplied by the cross-sectional area of the pipe. Because we are only interested in obtaining a rough final value, the exhaust velocity need not be measured exactly. These values can be found in the table on the next page.

Determining the pressure drop through the chamber is somewhat more laborious. Representing the chamber as a circular pipe, we can calculate the pressure drop if we know the head loss. The head loss, in turn, is found with knowledge of the pipe geometry, flow characteristics, and moody friction factor, f . The friction factor can be determined through correlations relating it to the Reynolds number and surface roughness, ϵ , which can be found in tables.⁸⁶

⁸⁴ Russo, S; Gomez, A. "Experimental Study of Laminar Spray Flames at Moderately High Pressures". Doctoral Dissertation. Yale University, Dec. 2002.

⁸⁵ Beranek, LL. *Acoustics*. McGraw-Hill: 1954.

⁸⁶ White, F. *Fluid Mechanics, 5th Edition*. McGraw-Hill: 2003.

$$\text{Re}_d = \frac{\rho v d}{\mu} \quad (\text{Eq. 4})$$

$$\frac{1}{f^{1/2}} \approx -1.8 * \log \left[\frac{6.9}{\text{Re}_d} + \left(\frac{\varepsilon/d}{3.7} \right)^{1.11} \right] \quad (\text{Eq. 5})^{86}$$

$$h_f = f \frac{L}{d} \frac{v^2}{2g} \quad (\text{Eq. 6})$$

$$\Delta p = \rho g (h_f + z_2 - z_1) \quad (\text{Eq. 7})$$

Where z_2 and z_1 are the final and initial height of the pipe.

Although the final chamber varied in cross-sectional area, it is represented here as having a constant diameter of 8” for simplicity. The length is the total of the chamber length and chimney height. Exhaust gas is obviously made up of many different compounds. Because carbon dioxide is a major component, we have used CO₂’s density and viscosity.

$\rho(\text{CO}_2 \text{ at } 20^0\text{C}) =$	1.83 kg/m ³
$\mu(\text{CO}_2 \text{ at } 20^0\text{C}) =$	1.48*10 ⁻⁵ N*s/m ²
$d =$.2032 m
$v(\text{exhaust}) \sim$	5 m/s
$v(\text{at } 8'') =$.31 m/s
$\varepsilon (\text{riveted steel})^3 =$	3.0*10 ⁻³ m
$L =$	2.5 m
$z_2 - z_1 =$	1.5 m

$\text{Re}_d =$	7800
$f =$.049
$h_f =$	3.0*10 ⁻³ m

$\Delta p =$	27 N/m ²
--------------	---------------------

We see that the head loss is very small with this set-up, and is negligible compared to the change in height. Had we represented the entire chamber as 3”flexible tubing, and used a higher roughness value to match, we could obtain a head loss on the order of 2 m, which would basically double our calculated pressure loss

Plugging the necessary values into Equation 3, we calculate a total volume of 40 m³ (with a head loss of 2 m, V = 17 m³). Clearly a chamber of this size would be impossible to attach to the truck, and it seems there must be other factors at work that are not considered here. In reality, a dampening chamber of approximately 0.1 m³ proved to be sufficient for our purposes.

Our estimation here represented the entire chamber as one long pipe, when in reality, this is not the case. The turning of the exhaust as it goes through the tubes, as well as the 90⁰ direction change upon entering the chimney surely help to increase flow resistance through the chamber. Even more importantly, our model did not take into account the mixing of the exhaust streams coming from each tailpipe. This mixing undoubtedly creates a strong buffering effect for the pulses, and is likely what allows us to get away with a much smaller volume than estimated.

APPENDIX E: IMAGES



Image 1: The Dampening Chamber



Image 2: Connecting to the tailpipe



Image 3: The probe is in place



Image 4: HC set-up



Image 5: The Test Tank



Image 6: Under the Hood



Image 7: The Vegetable Oil Tank



Opacity Meter